# 博 士 論 文
# （Doctoral Thesis）

# Characterization of tobacco plants with the hyper-galactosylated cell wall components

# 高ガラクトシル化された細胞壁をもつタバコ植物の性状解析

2018

Department of Molecular Biotechnology

Graduate School of Advanced Sciences of Matter

Hiroshima University

Tayebeh Abedi

# 目　　次

# (Contents)

# 主　論　文

# （Main Thesis）

# Table of Contents

# Chapter 1. Preface

All plant cells are surrounded by rigid and semi penetrable layers named cell wall. This complex extracellular matrix is the significant material that causes a main structural difference between plant and animal cells (1). Plant cell wall which contains carbohydrates and proteins affects plant characteristics and growth via its several essential functions in plants (2). In molecular terms, the cell wall is highly dynamic which modifies during growth and development dependent on cell type and cell functions in the plant (3).

Plant cell wall categorized to the primary and secondary cell wall. All plant cells are surrounded by primary cell wall composed of cellulose, hemicellulose and pectin. Primary cell wall controls cell morphology via controlling cell growth direction. On the other hand, secondary cell wall composed of cellulose, hemicellulose and lignin is added to some kinds of mature cells such as xylem fiber cells to support their functions (4). From different studies, interaction and interconnection among cell wall polymers lead to cell wall integrity besides its flexibility (5, 6). Therefore, studying of cell wall composition is fundamental for understanding cell wall biosynthesis and remodeling impacts on plant life cycle via the biological function of cell wall such as signaling properties. However, little is known about the function of the individual cell wall matrix components in cellular signaling (7).

Cell wall polymers mostly compose of polysaccharides and the simple sugars are generally found in different plant tissues in variable proportion. UDP-Galactose (UDP-Gal) is one of the most important nucleotide-sugar precursors which is used in assembling of cell wall polymers, through cell wall galactosylation processes in Golgi body. Among cell wall polymers, pectin and hemicellulose as non-cellulosic part of the cell wall (so-called cell wall matrix components) are galactosylated (5, 8, 9).

Essential factors involved in cell wall matrix galactosylation are galactosyltransferases (GalTs), UDP-galactose epimerases (UGE) and UDP-galactose transporters (UGT). UGE is an $NAD^+$ dependent enzyme that interconverts UDP-Gal

from/to UDP-glucose (UDP-Glc) in the cytosol (10). Then this UDP-Gal would be transported from cytosol to the Golgi apparatus by the essential function of UGTs, the main transporters which located in the membrane of the Golgi body (11). Finally, in the Golgi lumen, GTs would use these UDP-Gal as a substrate for synthesis of pectin and hemicellulose polymers (9, 12).

One of the key prospective research areas in plant cell wall is to study the relationship between the structural complexity and variation of cell wall polymers and their subsequent biological function such as altered mechanical stiffness in plants. In our laboratory, Khalil et al., previously reported that tobacco plants transformed with the human UDP-galactose transporter 1 gene (*hUGT1*), the first isolated UDP-galactose transporter which is a typical model for UDP-galactose transporter, displayed several morphological and physiological alterations, such as enhanced growth, increased accumulation of chlorophyll and lignin, a gibberellin-responsive phenotype, and an increased proportion of Gal in arabinogalactan proteins (13).

The aim of my thesis is a study on *hUGT1*-transgenic tobacco plants, to investigate the influence of the expression of this UDP-Gal transporter on cell wall matrix hyper-galactosylation. Afterward, I aimed to examine that the cell wall hyper-galactosylation impacts on plants phenotypic and physiological characteristics which might result from signaling activity of cell wall components.

My thesis is started by chapter 2 with a general introduction involved some basic and essential information about plant cell wall. Since the main material of my study was plant cell wall, it has been really important to begin this thesis with a brief introduction of cell wall.

In chapter 3, I examined a hypothesis that extra transportation of UDP-Gal from cytosol to Golgi by *hUGT1* expression might lead to an alteration of cell wall monosaccharide composition. The monosaccharide composition of cell wall matrix of leaf and stem in *hUGT1*-transgenic and control plants was analyzed. Generally, HPLC analysis revealed the alteration of monosaccharide composition in pectin and hemicellulose. In particular, Gal ratio in total sugar composition of cell wall

dramatically elevated in the hemicellulose II and pectin fraction in the *hUGT1*-transgenic plants. Furthermore, oligosaccharide mass profiling (OLIMP) revealed that xyloglucan (XG) is the main acceptor of Gal in hemicellulose II. Since the degree of galactosylation in XG would be related to the mechanical strength of primary cell wall, the hyper-galactosylation of XG might elevate the rigidity of tobacco plants. Moreover, an increased Gal tolerance was shown in the *hUGT1*-transgenic plants. The enhanced stream of Gal from cytosol to Golgi body by hUGT1 and consequent incorporation of this extra Gal into cell wall component seemed to lead to the increased Gal tolerance.

In chapter 4, I proposed hyper-galactosylation of Gal-containing cell wall polysaccharides via the expression of *hUGT1* might have an important impact on plant growth and development such as plant hardness. Strength test for stem and leaf of *hUGT1*-transgenic and control plants determined by breaking and bending tests revealed an increased rigidity in leaf and stem of transgenic plants. This result suggested that the hyper-galactosylated side chains of XG were involved in the increased strength of cell wall. Subsequent transmission electron microscopic analysis supported the cell wall thickness in leaves palisade cells and those of cortex cells and xylem fibers in the stem. Besides, the biomass and total cell wall content were measured. The biomass and total cell wall materials extracted from the leaves and stems of *hUGT1*-transgenic plants were higher than those of control plants. These results supported the increased cell wall thickness. In addition, the cell walls of the *hUGT1*-transgenic plants showed increased lignin contents, which was supported by the up-regulation of some genes encoding enzymes which are rate-limiting in lignin biosynthesis. From these results, although a possibility of hyper-galactosylation of XG is ruled out, the increased rigidity of *hUGT1*-transgenic plants are mainly caused by the increased cell wall thickness and the enhanced lignin accumulation.

# Chapter 2. General introduction

## 2.1. Plant Cell wall

Plants have a special ability to convert light energy to chemical energy utilized in the conversion of inorganic carbon to organic forms and produce simple sugars that play an important role in cell survival as energy sources or as structural components of cell walls, membranes, and glycoproteins. Most of these photosynthetically fixed carbons are incorporated into cell wall carbohydrates; the rest forms glycoproteins, glycolipids and storage polysaccharides (14).

Plant cell wall is positioned on the outer layer of the cell next to cell membrane (1). This rigid and supportive layer protects cells and gives them special shape by controlling the direction of cell growth. Although cell wall containing pores allow molecules and signals to pass between individual plant cells, it acts as a barrier to protect the cell against pathogens and plant viruses (9). The cell wall polysaccharides would carry important information for cell signalling processes (7). In addition, plant cell wall is important sources of industrial raw materials for textile fibers, paper, and wood products, and potentially for renewable biofuels or as a nutrition source for humans and animals (15, 16).

## 2.2. Plant cell wall structure

The plant cell wall is multi-layered, and up to three layers may be found in plant cell walls depending on the cell type and its developmental stage. The outer layer from plasma membrane is middle lamella which keeps near cells together. Then, in all growing plant cells, a thin and flexible primary cell wall layer is formed between the plasma membrane and middle lamella. Finally, the last thick and rigid layer named secondary cell wall is deposited between the plasma membrane and primary cell wall in some particular plant cell types after ceasing of their dividing and growing (Fig. 2.1). While all growing plant cells have a middle lamella and primary cell wall, the

secondary cell wall is not found in all cell types. Specialized and matured cells such as vessel elements or fiber cells are surrounded by a secondary cell wall. (3)

The composition and function of each layer vary in different species depending on cell types and developmental stages, which shows a relationship between cell functional properties and its cell wall composition and structure (4). The primary cell wall is comprised of cellulose microfibrils embedded within a matrix of hemicellulose and pectin polysaccharides. The pectic polysaccharides include homogalacturonan, and rhamnogalacturonan I and II (5, 8) and the hemicellulosic polysaccharides include xyloglucans, glucomannans, xylans, and mixed-linkage glucans (3).While the strength of primary cell wall supports cell structure, its flexibility allows cells to expand and elongate. Once the cells have reached their final size, the secondary cell wall composed of cellulose, hemicelluloses and lignin is accumulated inside the primary cell wall. This thick secondary cell wall containing lignin provides mechanical support in fiber cells as well as strengthening and waterproofing the wall of xylem cells in vascular tissue (6). Besides polysaccharides components plant cell walls also contain many proteins and glycoproteins (2). For example, arabinogalactan proteins are complex molecules found on the plasma membrane and in the cell wall with important roles in plant growth and development via possible signaling events at the cell surface (3).

### 2.3. Plant cell wall biosynthesis

According to the analysis of complete genomes a large portion of genes, more than 2000 genes of plants, are expected to be related to the biosynthesis and remodeling of plant cell wall components (17, 18, 19). For example in Arabidopsis, 15% of the genes have been identified to cooperate in these processes (20). It is well known that plant cell wall biosynthesis is done in multiple cellular compartments (3). While cellulose microfibrils are synthesized at the plasma membrane by cellulose synthase complexes (CSCs), the cell wall matrix polysaccharides (pectin and hemicelluloses) as non-cellulosic part of plant cell wall are synthesized in the Golgi apparatus. Such non-cellulosic polysaccharides are transported to the cell surface through the intermediacy of within Golgi-derived vesicles which fuse with the cell membrane to incorporate into the cell wall (3, 5, 8).

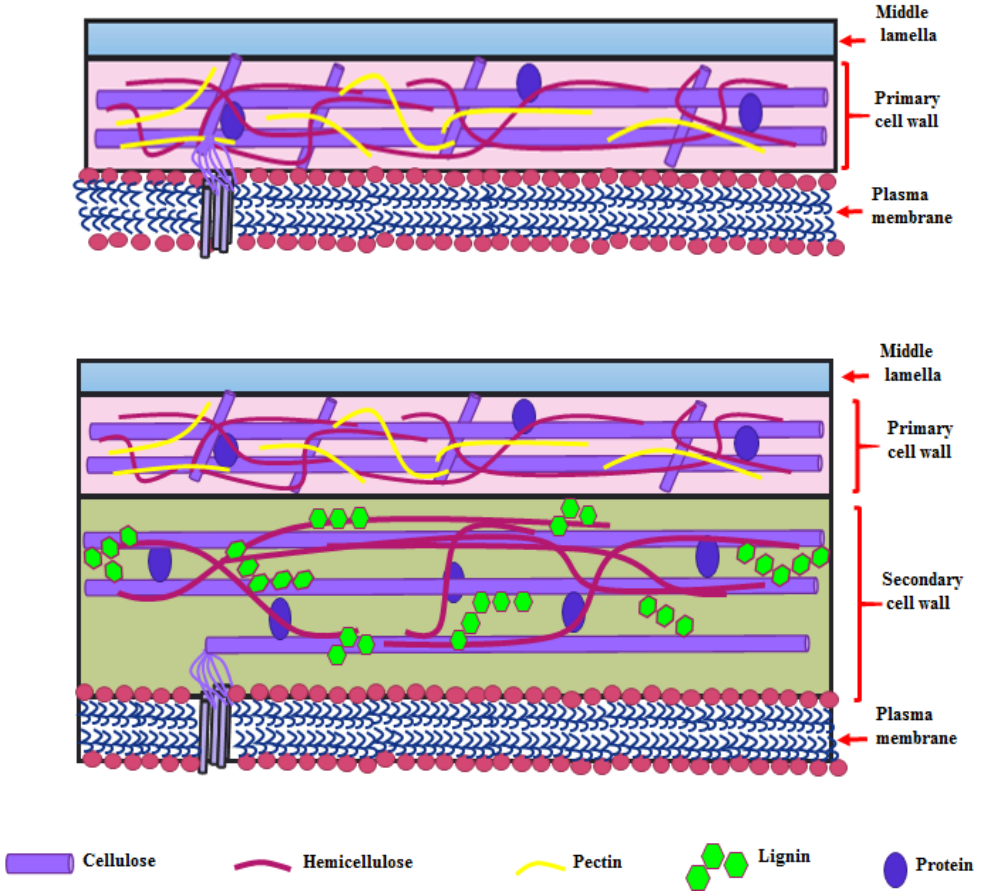


**Fig 2.1.** Plant cell wall structure

The enzymatic process that attaches an oligosaccharide side chain to lipids, protein or other organic molecules is known as glycosylation. This process is the most common posttranslational modification of proteins that occurs in ER and Golgi apparatus (21). Galactose is incorporated into the pectin such as rhamnogalacturonan-I and -II, and the hemicelluloses such as xyloglucan, which contain galactose residue (8, 22), in Golgi apparatus via the function of different kinds of essential enzymes known as galactosylation process (3, 5, 8, 9).

Sugars cannot be used as building blocks for cell components as long as being activated. Nucleotide diphosphate sugars (NDP-sugars) are activated forms which contain the required energy for the assembly of their sugar moiety on appropriate cell component (23). UDP-sugar pyrophosphorylase (USPase; EC 2.7.7.64), which is localized in the cytosol, catalyzes a reversible transfer of the uridyl group from UTP to sugar-1-phosphate, producing UDP-sugar and pyrophosphate (PPi) (10). The schematic process of UDP-glucose (UDP-Glc) synthesis is shown in Figure 2.2.

In plants, galactosylation of non-cellulosic cell wall polysaccharides in Golgi apparatus requires UDP-galactose (UDP-Gal) as a precursor, which is synthesized from UDP-glucose (UDP-Glc) by the action of uridine 5'-diphospho-galactose-4-epimerase (UGE) in the cytosol (24). It has been reported that a large family of nucleotide sugar transporters (NSTs), as integral-membrane proteins that possess 6–10 transmembrane domains which range from 45 to 55 kDa in size, is localized in Golgi apparatus membrane (11, 25). UDP-galactose transporter (UGT) provides a link between the synthesis of UDP-Gal in the cytosol and the galactosylation process in the Golgi lumen (11). Furthermore, another important factor in galactosylation is galactosyltransferase (GalT) that catalyzes the formation of glycosidic linkages between an activated sugar moiety (UDP-Gal) and a specific polysaccharide acceptor. GTs are thought to be localized in the Golgi lumen (12). As it is shown in Figure 2.3, the synthesis of matrix polysaccharides in Golgi apparatus requires the cooperation of three different kinds of essential factors (UGEs, NSTs, and GTs). Finally, products accumulated in Golgi lumen are transported to the cell wall via vesicles (3, 9).

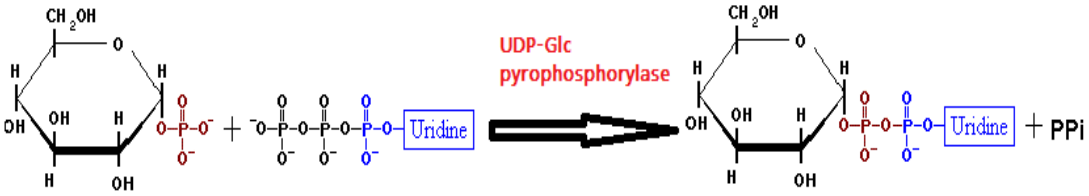


**Figure 2-2.** UDP-Glc pyrophosphorylase activity in UDP-Glc synthesis

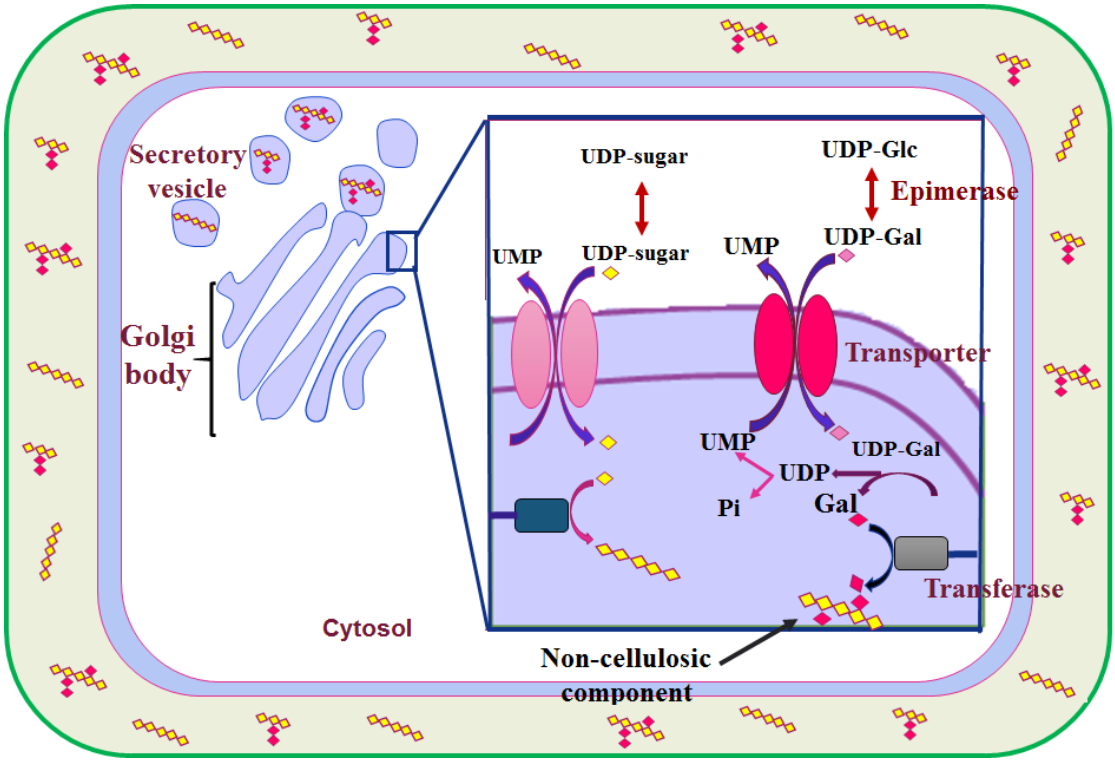


**Fig 2.3.** The cell wall matrix polysaccharides (pectins and hemicelluloses) are synthesized in the Golgi apparatus and transported to the cell surface via Golgi-derived vesicles

# Chapter 3. Characterization of plants with the hyper-galactosylated cell wall components

## 3.1. Introduction

Cell wall materials (CWMs) play essential roles not only in plant growth and development but also in the response of plants to the environment and in their interactions with symbionts and pathogens (26). There are two types of cell walls, primary and secondary. Primary cell walls are deposited during cell growth and consist mainly of polysaccharides that can be broadly classified as cellulose, cellulose-binding hemicelluloses, and pectins. The latter two classes of cell wall components are often referred to as matrix polysaccharides, which are synthesized within Golgi cisternae, whereas cellulose is generated at the plasma membrane in the form of paracrystalline microfibrils (27,15). Secondary cell walls are deposited between the primary cell wall and the plasma membrane in confined locations where great mechanical strength and structural reinforcements are required, such as the xylem, and are produced after primary cell wall deposition and cell expansion are completed.

In the Golgi apparatus, glycosyltransferases catalyze the glycosidic linkages between a sugar moiety and specific polysaccharide acceptor, resulting in various sugar chain formations (28). Nucleotide sugar transporters (NSTs) are indispensable because they incorporate substrates used in the biosynthesis of matrix polysaccharides into the Golgi lumen as glycosyltransferase partners (14). Genes that encode NST family proteins are widely found in eukaryotic organisms and have been isolated from animal, plant, and yeast cells (29). Among the NST family of proteins, UDP-galactose (UDP-Gal) transporters are involved in transporting UDP-Gal into the Golgi lumen (29). UDP-Gal transporters have been described in mammals, *Drosophila*, *Caenorhabditis elegans*, *Entamoeba*, *Giardia*, *Leishmania*, yeast, and other organisms (30). Plant UDP-Gal transporters have been reported in *Arabidopsis* (12) and rice (31). The *Arabidopsis* UDP-Gal/UDP-glucose (UDP-Glc) transporter AtUTr1 and UDP-Gal transporter AtUTr2 have been isolated and characterized (32, 33). Subsequently, two additional

UDP-Gal transporters, AtUDP-GalT1 and AtUDP-GalT2, were identified (34), and the recombinant protein AtNST-KT1 was functionally characterized as a UDP-Gal transporter (35). Furthermore, three UDP-Gal transporters have been isolated from *Oryza sativa* (31).

Recently, Zhang et al. (36) and Song et al. (37) reported that an UDP-Glc transporter of rice, OsNST1, modulates cell wall biosynthesis. The *bc14* mutant harbors a mutation in *OsNST1*, which shows reduced mechanical strength owing to decreased cellulose content and altered wall structure. These findings indicate that absence of or a defect in NSTs strongly perturbs the supply of substrates, thus affecting polysaccharide biosynthesis and cell wall matrix composition. Although NSTs are likely to contribute to carbohydrate production outside the plasma membrane of plant cells, the machinery involved in this reaction is not fully understood.

In previous work, Khalil et al., described the characteristics of tobacco plants transformed with the human UDP-Gal transporter 1 gene (*hUGT1*; 38), designated *hUGT1*-transgenic tobacco plants (13). *hUGT1* is the first mammalian nucleotide sugar transporter for which a cDNA sequence was identified (38), and the important amino acid residues composing transmembrane domains and UDP-Gal recognition sites have been thoroughly analyzed (39). Although a number of plant UGTs have been identified (12,31–35), they chose *hUGT1*, as the best-studied UGT, for their investigations. In a previous report (13), they demonstrated that *hUGT1* was transcribed and translated in transgenic tobacco plants and that hUGT1, which showed UDP-Gal transporter activity, was mainly localized to the trans-Golgi network and endoplasmic reticulum in tobacco cells, similar to human cells (13). These transformants displayed enhanced growth during cultivation in soil and axillary shoots showed an altered determinate growth habit. Although the *hUGT1* expression level and UDP-Gal transport activity were not strongly correlated with growth and morphology among the *hUGT1*-transgenic tobacco plants examined, line 23 showed the strongest phenotype described above (13). Increased leaf thickness, caused by an increased amount of spongy tissue, increased numbers of xylem vessels in the stem, increased accumulation of lignin and chlorophyll, and hyper-galactosylated arabinogalactan proteins were observed in *hUGT1*-transgenic

plants.

Polysaccharides in the plant cell wall not only provide physical support but are also signaling substances. For example, oligosaccharides derived from some Gal-containing polysaccharides, such as xyloglucan and galactoglucomannan, have biological activities (40–44). In addition, arabinogalactan proteins play a crucial role in various physiological functions in plant cells (45). Thus, changes in Gal-containing cell wall polysaccharides might have an important impact on plant growth and development.

Hyper-galactosylation of cell wall matrix polysaccharides has been successfully achieved by introduction of an UDP-Glc/Gal epimerase gene into potato (46) and a galactosyltransferase gene into *Arabidopsis* (47). However, the introduction of an UDP-Gal transporter has not been reported previously. Given that plant cell wall matrix polysaccharides are synthesized in the Golgi apparatus, an UDP-Gal transporter must play a key role in linking UDP-Gal biosynthesis in the cytosol and galactosylation of polysaccharides in the Golgi apparatus. I hypothesized that increased UDP-Gal transport activity will drastically affect cell wall matrix polysaccharide structure. In this study, I revealed that enhanced UDP-Gal transport activity caused by *hUGT1* expression altered the monosaccharide composition of the cell wall matrix components of *hUGT1*-transgenic plants. In particular, I focused on the increase in the ratio of galactose to total monosaccharide residues, so-called “hyper-galactosylation”, in the cell wall matrix of transgenic plants. I also showed that the additional UDP-Gal transport activity increased the tolerance to galactose, which may be toxic to plant cells. The dynamic change in cell wall polymer composition caused by hyper-galactosylation of cell wall matrix polysaccharides is discussed.

### 3.2. Materials and methods

#### 3.2.1. Plant materials and growth conditions

As reported previously (13), tobacco (*Nicotiana tabacum* cv. SR-1) plants were transformed with *hUGT1* (38), together with a hemagglutinin tag inserted between the CaMV *35S* promoter and a nopaline synthase gene (*nos*) terminator, designated pBIN-hUGT1. The transformation was mediated by *Agrobacterium tumefaciens* strain LBA4404. As a control, tobacco plants were transformed with the empty vector pBIN19. The pBIN19- and *hUGT1*-transgenic tobacco plants were cultured *in vitro* for 1 month, then transferred to soil in pots and cultivated with the addition of 1:1000 diluted Hyponex fertilizer (Hyponex Japan, Osaka, Japan) at 25°C with a 16-h photoperiod under a fluorescent daylight lamp (50 μmol/$m^2$/s) in a climate-controlled room. After growth in the soil for 2 months, the pBIN19- and *hUGT1*-transgenic tobacco plants were harvested and used as a material for CWM extraction.

#### 3.2.2. Extraction of CWM

To extract CWM from a large number of plant samples, a simplified method devised by Foster et al. (48) was employed with several modifications. The eleventh leaf or tenth stem internode from the shoot apex of harvested plants were used for CWM extraction. Air-dried plant material (60 mg) was ground with 5-mm stainless balls in a 2-mL screw cap tube (Watson, Tokyo, Japan) using a bead crusher μT-12 (Taitec Corp., Saitama, Japan) at 2,600 rpm for 1 min. The homogenate was washed in 1.5 mL of 70% ethanol, centrifuged at 9700 × *g* for 10 min, and the supernatant was removed. The pellet was resuspended in 1.5 mL chloroform/methanol [1:1 (v:v)], centrifuged at 9700 × *g* for 10 min, and the supernatant was removed. The pellet was resuspended in 500 μL acetone, and the solvent was evaporated. To remove starch, the sample was resuspended in 1.5 mL of 0.1 M sodium acetate buffer, pH 5.0, and incubated for 20 min at 80°C. The sample was mixed with a reagent mixture comprising 35 μL of 0.01% $NaN_3$, 35 μL α-amylase (50 μg/mL $H_2O$; from *Bacillus* species; Sigma-Aldrich Corp., St Louis, MO,

USA), and 17 μL pullulanase (18.7 units from *Bacillus acidopullulyticus*, Sigma-Aldrich Corp.), and incubated overnight at 37°C with moderate mixing. After incubation, the sample was heated for 10 min at 100°C, centrifuged at 9700 × *g* for 10 min, and the supernatant was discarded. The pellet was washed three times with 1.5 mL distilled water, resuspended in 500 μL acetone, and air dried. The residue was defined as the CWM.

### 3.2.3. Extraction and fractionation of leaf CWM

The eleventh leaf from the shoot apex of harvested plants was used for leaf CWM extraction. Leaves of the pBIN19- and *hUGT1*-transgenic plants (1 g) were ground to a powder in liquid nitrogen with a mortar and pestle. The powder was homogenized in ice-cold 250 mM potassium phosphate buffer (pH 7.0) with a Teflon homogenizer. The homogenate was centrifuged at 2000 ×*g* for 10 min at 4°C. The pellet was resuspended in ice-cold buffer and centrifuged. This step was repeated twice. The pellet was resuspended in ice-cold water and centrifuged at 2000 ×*g* for 10 min at 4°C, and then resuspended in ice-cold buffer and centrifuged. This step was repeated three times. Next, the pellet was suspended in a 10-fold volume of methanol and incubated for 30 min at 80°C. After centrifugation at 2000 ×*g* for 10 min at 4°C, the supernatant was discarded, and the pellet was resuspended in methanol and centrifuged again. The supernatant was discarded, and the pellet was resuspended in ice-cold water and centrifuged at 2000 ×*g* for 10 min at 4°C. The supernatant was discarded. To remove starch, the pellet was incubated in 10 volumes of α-amylase solution (0.1 mL α-amylase Type I-A; Sigma-Aldrich Corp.) in 100 mL of 20 mM sodium phosphate buffer, pH 7.0, containing 6 mM NaCl for 24 h at 28°C. After centrifugation at 2000 ×*g* for 10 min at 4°C, the pellet was washed twice with ice-cold water. After the resuspension and centrifugation, the pellet, defined as a leaf CWM, was recovered.

To extract the pectin fraction, 50 mM EDTA solution (50 mM EDTA, 50 mM acetate-sodium acetate buffer, pH 4.5) was added to the leaf CWM and incubated for 4 h at 100°C. After centrifugation at 1000 ×*g* for 10 min, the supernatant was recovered

(supernatant-1). Next, 20 mM EDTA solution (20 mM EDTA, 50 mM acetate-sodium acetate buffer, pH 4.5) was added to the pellet and homogenized with a Teflon homogenizer, and then the same incubation and centrifugation steps were carried out. The supernatant (supernatant-2) was recovered and combined with supernatant-1, and then dialyzed with water for 48 h at 4°C to yield the pectin fraction. To extract the hemicellulose I fraction, the pellet obtained above was resuspended in 1 M KOH/20 mM $NaBH_4$ solution and incubated for 24 h at 28°C. After centrifugation at 1000 ×*g* for 10 min, the supernatant was recovered and dialyzed with water for 48 h at 4°C to yield the hemicellulose I fraction. To extract the hemicellulose II fraction, the pellet obtained above was resuspended in 4 M KOH/20 mM $NaBH_4$ solution and incubated for 24 h at 28°C. After centrifugation at 1000 ×*g* for 10 min, the supernatant was recovered and dialyzed with water for 48 h at 4°C to yield the hemicellulose II fraction.

To quantify each cell wall fraction, the orcinol–sulfuric acid method (49) was employed. A colorimetric analysis was carried out by measuring the absorbance at 600 nm.

### 3.2.4. Extraction and fractionation of stem CWM

Isolation of CWM from stems of the pBIN19- and *hUGT1*-transgenic plants was performed as described by Selvendran and O'Neill (50) with a slight modification. The entire stem from harvested plants was used for stem CWM extraction. In total, 25 g (fresh weight) of stems were ground with a mortar and pestle in liquid nitrogen, blended with 100 mL (twice the volume of the material) of 1.5% SDS solution containing 5 mM $Na_2S_2O_5$ in a Waring blender, and subsequently homogenized with Ultraturrax (IKA Works GmbH & Co., Staufen, Germany). The homogenate was washed twice with a double volume of 0.5% (w/v) SDS solution containing 3 mM $Na_2S_2O_5$, and then crushed in the same solution in a pot mill containing ceramic balls at 60 rpm for 15 h at 4°C. The crushed residue was recovered and washed twice in 100 mL distilled water by suspension and centrifugation. The pellet was resuspended in 90% DMSO and incubated overnight at room temperature to remove starch. After centrifugation, the

pellet was resuspended in 90% DMSO and incubated for 1 h at room temperature, and then washed five times with distilled water. The pellet was resuspended in a small volume of distilled water and dialyzed overnight at 4°C in distilled water. The pellet was recovered using centrifugation and stored at −20°C as a CWM.

To obtain the pectin I fraction (the 1,2-diaminocyclohexanetetraacetic acid (CDTA)-soluble pectin), ~1 g of CWM was extracted using 50 mM CDTA solution, pH 6.5 (CDTA disodium salt, Sigma-Aldrich Corp.). After centrifugation, the supernatant was recovered and concentrated in an evaporator. The fraction was dialyzed overnight at 4°C in distilled water and stored at −20°C. To obtain the pectin II fraction ($Na_2CO_3$-soluble pectin), the CDTA-insoluble residue was extracted in 50 mM $Na_2CO_3$/20 mM $NaBH_4$ solution, pH 10.8. After centrifugation, the supernatant was recovered and concentrated in an evaporator. The fraction was dialyzed overnight at 4°C in distilled water and frozen at −20°C.

To obtain the hemicellulose I fraction (the 1 M KOH-soluble hemicellulose), the pellet obtained in the previous step was extracted three times in 1 M KOH/20 mM $NaBH_4$ solution under $N_2$ gas. After each centrifugation, the supernatants from the extractions were recovered, combined, and filtered using a GF/C glass filter. The filtrate was adjusted to pH 5.0 by acetic acid, concentrated, dialyzed in deionized water, and frozen at −20°C.

To obtain the hemicellulose II fraction (the 4 M KOH-soluble hemicellulose), the pellet obtained in the previous step was extracted three times in 4 M KOH/20 mM $NaBH_4$ solution under $N_2$ gas. After each centrifugation, the supernatants from the extractions were recovered, combined, and filtered using a GF/C glass filter. The filtrate was adjusted to pH 5.0 by acetic acid, concentrated, dialyzed in deionized water, and frozen at −20°C.

The quantification of each cell wall fraction was performed using the orcinol–sulfuric acid method as described above.

### 3.2.5. Relative proportion of monosaccharides in CWMs and cell wall matrix fractions

To analyze the monosaccharide composition, 1 mg CWMs or 2 μg of the pectin and hemicellulose fractions extracted from leaves and stems of the pBIN19- and *hUGT1*-transgenic tobacco plants were used. Each sample was hydrolyzed to release monosaccharides in 2 M trifluoroacetic acid (TFA) solution. The released monosaccharides were fluorescently labeled using a *p*-aminobenzoic ethyl ester (ABEE) labeling kit (J-Oil Mills, Inc., Tokyo, Japan) in accordance with the manufacturer's instructions. L-arabinose (Ara), L-fucose (Fuc), D-galactose (Gal), D-galacturonic acid (GalA), D-glucose (Glc), D-glucuronic acid (GlcA), D-mannose (Man), L-rhamnose (Rha), and D-xylose (Xyl) were used as a standard mixture of the monosaccharides found in the cell wall. The ABEE-labeled monosaccharides were analyzed using a high-performance liquid chromatography (HPLC) 880 system (Jasco Co., Tokyo, Japan) with a Honenpak C18 column (75 mm × 4.6 mm, J-Oil Mills, Inc) at 30°C and an FP-1520S Intelligent Fluorescence Detector (Jasco Co.). The HPLC conditions were as follows: mobile phase, 0.2 M potassium borate buffer (pH 8.9)/acetonitrile [93:7 (v:v)]; flow rate, 1.0 mL/min; fluorescence detection, excitation at 305 nm, and emission at 360 nm (51). In a preliminary experiment, the proportion of GalA in the leaf pectin fraction calculated from the corresponding peak areas of HPLC were extremely low compared with that in the pectin fraction isolated from the leaf mesophyll of *N. tabacum* described in a previous report (85.7% as uronic acid; 52). The reduced GalA proportion seemed to be caused by the low ABEE-labeling efficiency for GalA. Because such a difference in the ABEE-labeling efficiency might be observed for all monosaccharides, the ABEE-labeling efficiency of each monosaccharide was estimated using the same concentration (200 μM) of standard monosaccharides that are assumed to be released from CWMs. As expected, the ABEE-labeling efficiency of each monosaccharide was different, so the peak area value was corrected by the ABEE-labeling efficiency. Because Glc showed the highest labeling efficiency with ABEE, the relative labeling efficiencies of the other monosaccharides at the same concentration were calculated (Glc defined as 100%). The labeling efficiency of each monosaccharide was as follows: Ara, 98.7%; Fuc, 76.5%; Gal, 91.1%; GalA, 5.3%; Glc, 100%; GlcA, 24.6%; Man,

92.2%; Rha, 61.1%; and Xyl, 85.2%. The relative proportion of each monosaccharide in the CWMs and cell wall matrix fractions was calculated from the peak area corresponding to each monosaccharide.

### 3.2.6. Oligosaccharide mass profiling (OLIMP)

To analyze the galactosylation of xyloglucan, the OLIMP (53) method was employed with some modifications. A total of 25 μg freeze-dried leaf hemicellulose II was resuspended in 50 μL of 100 mM sodium acetate-acetate buffer, pH 5.5, and 0.2 U of xyloglucanase (E-XEGP, EC 3.2.1.151, CAZY Family: GH5, Megazyme International, Wicklow, Ireland) was added. Then, 25 μg of tamarind xyloglucan (P-XYGLN, Megazyme) used as the xyloglucan standard was also resuspended in the same buffer containing E-XEGP. The mixture was incubated for 16 h at 40°C. After centrifugation, the supernatant (10 μL) of the digested sample was recovered. To remove salts, BioRex MSZ 501 cation exchange resin beads (Bio-Rad, Hercules, CA, USA) were added to the sample and incubated at room temperature for 15 min. For the matrix and target plates, 10 mg/mL 2,5-dihydroxybenzoic acid (DHB) in water and DE1580TA (Kratos, Shimadzu, Kyoto, Japan) were used, respectively. The target plate spotted with DHB and sample mixtures was placed into a MALDI-TOF-quadrupole ion trap (QIT) mass spectrometer (AXIMA-QIT, Shimadzu). The machine was set to positive mode and the selected mass range was 750–3000 Da. Ions representing specific xyloglucan fragments were identified by their mass-to-charge ratio (m/z). The ion intensities (% area) of expected enzyme-digested xyloglucan fragments were summed to 100%, representing the relative abundance of each fragment.

### 3.2.7. Galactose tolerance assay

Surface-sterilized pBIN19- and *hUGT1*-transgenic tobacco seeds were sown on Murashige and Skoog (MS) solid medium (54) containing 100 mg/L kanamycin. One

week after sowing, germinated seedlings were transferred to 100 mL MS solid medium containing 0, 0.1, 0.2, 0.3, 0.4, 0.5, or 0.6% Gal in a 500-mL glass culture bottle, and cultured at 25°C with a 16-h photoperiod under a fluorescent daylight lamp in a culture room. Two weeks after transfer, plants were harvested to observe proliferation, the length of roots, and the monosaccharide content of the CWM. The assay was repeated three times to evaluate reproducibility.

### 3.2.8. Statistical analysis

Data were analyzed using one-way analysis of variance employing the *F*-test with $\alpha$ = 0.05 or 0.01 as the significance level.

## 3.3. Results

### 3.3.1. Altered monosaccharide composition in leaf cell wall polysaccharides of *hUGT1*-transgenic plants

I hypothesized that the altered composition of the monosaccharides, particularly galactose, in the cell wall of *hUGT1*-transgenic plants was caused by *hUGT1* overexpression and resulted in enhanced transport of UDP-Gal to the Golgi lumen. To test this hypothesis, the monosaccharide composition of CWMs from pBIN19- and *hUGT1*-transgenic plants was analyzed. The CWMs were hydrolyzed with 2 M TFA and the released monosaccharides were fluorescently labeled with ABEE. HPLC analysis revealed the presence of GlcA, GalA, Gal, Man, Glc, Ara, Xyl, Rha, and a trace amount of Fuc, in the leaf CWMs (Fig. 3.1A and 3.1B). To compare the monosaccharide composition in the leaf CWMs of pBIN19- and *hUGT1*-transgenic plants, the relative proportion of each monosaccharide detected was calculated from their peak area. In all of the monosaccharide analyses, the Glc peak area was not excessively high, indicating that starch was successfully removed using α-amylase. However, the low peak area of Glc, which is an abundant monosaccharide in cell walls, suggested that Glc was not completely released from the robust cellulose polymers in the CWMs using 2 M TFA.

Comparison of the monosaccharide compositions revealed that the relative proportions of GlcA, GalA, and Gal in the leaf CWMs of most *hUGT1*-transgenic plants were altered compared with those of pBIN19-transgenic plants (Table 3.1). In particular, all *hUGT1*-transgenic lines exhibited significantly higher Gal proportions compared with the pBIN19-transgenic plants (1.20- to 2.76-fold, Table 3.1). The leaf CWMs of *hUGT1*-transgenic plants contained a decreased proportion of GlcA, but an inverse correlation between the decreased proportion of GlcA and the increased proportion of Gal was not apparent. However, the alteration of the GalA proportion might be associated with the increased proportion of Gal because the percentages were inversely correlated. Interestingly, the total percentage of GalA and Gal was limited to 76–79% regardless of *hUGT1* expression. These results suggested that increased UDP-Gal transporter activity may have led to increased Gal content, as a proportion of leaf CWM

monosaccharides, and this influenced the GalA proportion. Therefore, further investigation to clarify the relationship between Gal and GalA proportions in the leaf CWMs was carried out.

To clarify which cell wall polymers in the *hUGT1*-transgenic plants were associated with the increased Gal proportion, CWMs isolated from the eleventh leaves of pBIN19- and *hUGT1*-transgenic plants were subdivided into pectin, hemicellulose I, hemicellulose II, and cellulose fractions (Table 3.2). The Gal content in the pectin and hemicellulose II fractions was directly influenced by the presence of hUGT1 in the Golgi apparatus of *hUGT1*-transgenic plants. A representative HPLC trace of ABEE-labeled monosaccharides in each polysaccharide showed that peaks corresponding to GlcA, GalA, Gal, Man, Glc, Ara, Xyl, and Rha were mainly detected in all fractions, although faint Fuc and some small additional monosaccharide peaks were observed.

In the pectin fraction, the proportions of GalA, Gal, and Rha in the pBIN19-transgenic control plants were consistent with those described in a previous report (55). The ratio of Gal to total monosaccharides in the *hUGT1*-transgenic plants was similar to or higher than that in pBIN19-transgenic control plants (Table 3.2). In particular, the Gal proportion of *hUGT1*-transgenic lines 4 and 23 was significantly higher (1.55- and 1.44-fold, respectively) than that of the control plants (Table 3.2). The pectin fraction contained homogalacturonan, rhamnogalacturonan-I (with pectic galactan, pectic arabinan, and type-I arabinogalactan side chains), rhamnogalacturonan-II, type-II arabinogalactan, and other polysaccharides. We previously reported that the type-II arabinogalactan bound to protein was hyper-galactosylated (13). My present results indicated that not only type-II arabinogalactan, but also other pectic fraction members containing galactose, were simultaneously hyper-galactosylated in the *hUGT1*-transgenic plants. The total percentage of GalA and Gal was limited to 58–60% in the pBIN19-transgenic control and *hUGT1*-transgenic plants (Table 3.2) and a similar limitation was observed in the leaf CWM samples (Table 3.1).

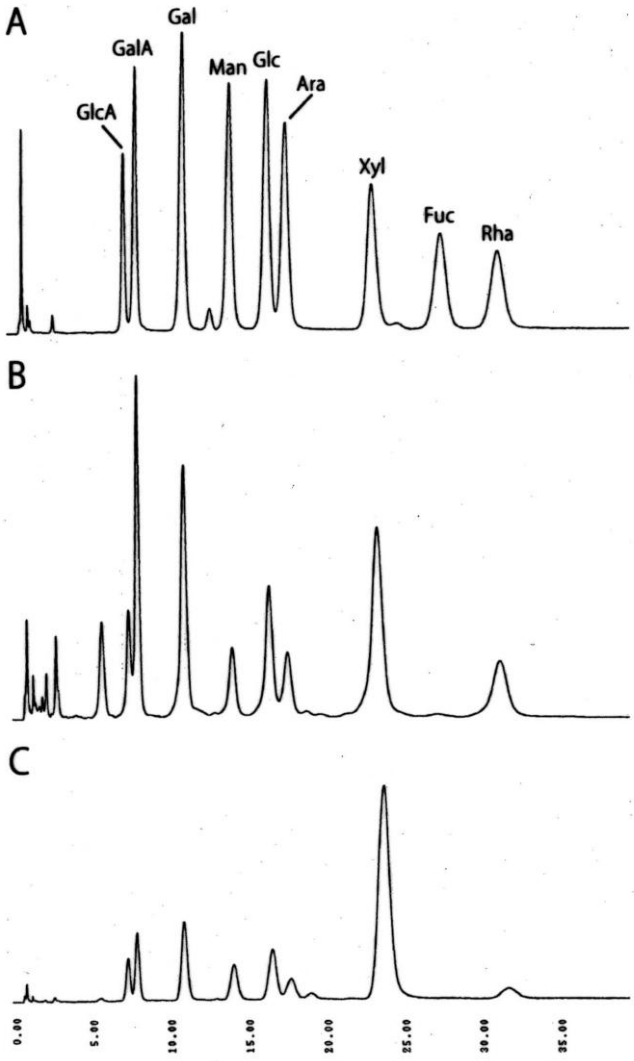


**Fig. 3.1.** HPLC traces of ABEE-labeled cell wall monosaccharides isolated from tobacco leaves and stems. (A) Standard monosaccharides. (B) Monosaccharides from cell wall material of pBIN19-transgenic control tobacco leaves. (C) Monosaccharide from cell wall material of pBIN19-transgenic control tobacco stems. Ara, L-arabinose; Fuc, L-fucose; Gal, D-galactose; GalA, D-galacturonic acid; Glc, D-glucose; GlcA, D-glucuronic acid; Man, D-mannose; Rha, L-rhamnose; and Xyl, D-xylose. Monosaccharaide concentrations were as follows; GlcA, 800 μM; GalA, 3200 μM; Ara, Fuc, Gal, Glc, Man, Rha, and Xyl, 200 μM. HPLC was performed using a Honenpak C18 column (75 mm × 4.6 mm) at 30°C, and ABEE-labeled monosaccharides were detected using a fluorescence detector. The HPLC conditions were as follows: mobile phase, 0.2 M potassium borate buffer (pH 8.9)/acetonitrile (93:7, v:v); flow rate, 1.0 mL/min; fluorescence detection, excitation at 305 nm, and emission at 360 nm.

**Table 3.1.** Monosaccharide composition of total cell wall polymers in leaves of pBIN19- and *hUGT1*-transgenic tobacco plants

| Monosaccharide | Mean ± standard deviation (%) | | | | |
|---|---|---|---|---|---|
| | pBIN19 | *hUGT1*-2 | *hUGT1*-4 | *hUGT1*-14 | *hUGT1*-23 |
| GlcA | 4.87 ± 0.90 | 3.21 ± 0.47 [b] | 3.17 ± 0.45 [b] | 4.42 ± 0.31 | 2.89 ± 0.57 [b] |
| GalA | 71.71 ± 0.52 | 70.06 ± 1.74 | 73.81 ± 1.39 | 62.37 ± 2.18 [b] | 68.10 ± 1.41 [a] |
| Gal | 4.89 ± 0.26 | 9.64 ± 0.38 [b] | 5.89 ± 0.04 [a] | 13.54 ± 0.32 [b] | 11.77 ± 0.74 [b] |
| Man | 1.30 ± 0.17 | 1.33 ± 0.14 | 1.07 ± 0.18 | 1.61 ± 0.0.28 | 1.50 ± 0.20 |
| Glc | 2.33 ± 0.52 | 2.29 ± 0.36 | 2.35 ± 0.52 | 2.30 ± 0.48 | 2.16 ± 0.42 |
| Ara | 1.94 ± 0.70 | 2.36 ± 0.77 | 2.34 ± 0.60 | 2.43 ± 0.88 | 2.74 ± 0.80 |
| Xyl | 9.14 ± 1.85 | 6.87± 2.33 | 6.94 ± 1.67 | 8.76 ± 2.04 | 6.18 ± 1.33 |
| Fuc | tra | tra | tra | tra | tra |
| Rha | 3.81 ± 0.54 | 4.24 ± 0.46 | 4.42 ± 0.54 | 4.58 ± 0.60 | 4.66 ± 0.13 |

[a]$P < 0.05$ and [b]$P < 0.01$.

GlcA, D-glucuronic acid; GalA, D-galacturonic acid; Gal, D-galactose; Man, D-mannose; Glc, D-glucose; Ara, L-arabinose; Xyl, D-xylose; Fuc, L-fucose; and Rha, L-rhamnose. Values in parentheses are the ratio of each monosaccharide (%) to total monosaccharides without glucose. The mean and standard deviation of at least three repeated analyses from three independent samples were calculated.

Homogalacturonan is the most abundant pectic polysaccharide, comprising ~65% of the pectin fraction, and a large portion of the constituent monosaccharides is GalA (56). On the other hand, rhamnogalacturonan-I represents 20–30% of the pectin fraction and is constituted of GalA, Rha, Gal, and Ara, with a notable amount of Gal contained in the side chains. Therefore, occupancy of the determinate cell wall space by homogalacturonan might have been diminished by accumulation of rhamnogalacturonan-I with Gal-containing side chains increased by the excess amount of Gal, resulting in the inverse correlation between Gal and GalA proportions in the pectin fraction. To clarify this possibility, the precise ratio of rhamnogalacturonan-I to homogalacturonan in the pectin fraction must be determined in a future study.

In the hemicellulose I fraction, xylan and/or glucuronoxylan were indicated to be abundant. No significant alteration in the ratio of Gal to total monosaccharides was observed, although the Glc content in all of the *hUGT1*-transgenic lines was higher (Table 3.2). The origin of Glc in this fraction might be callose (β-1,3-glucan), because no cell wall matrix polysaccharides containing Glc are extracted by 1 M NaOH.

In the hemicellulose II fraction, the ratio of Gal to total monosaccharides was also increased in the *hUGT1*-transgenic plants, whereas the GlcA, GalA, and Xyl proportions slightly decreased. In particular, the Gal proportion of *hUGT1*-transgenic line 23 was two-fold higher than that of the control plants (Table 3.2). The hemicellulose II fraction extracted with 4 M KOH contains xyloglucan, galactoglucomannan, and other polysaccharides, including, at times, tightly bound rhamnogalacturonan-I with pectic galactan and type-I arabinogalactan side chains (57), which are hyper-galactosylated candidates in the hemicellulose II fraction.

These results suggested that *hUGT1* expression in the plant cells enhanced the transport of UDP-Gal from the cytosol to the Golgi lumen for use in the production of non-cellulosic polymers with increased Gal incorporation, resulting in the alteration of the cell wall monosaccharide composition. Furthermore, the higher proportion of Gal in the *hUGT1*-transgenic plants (Table 3.1) originated from the increased incorporation of Gal in the pectin and hemicellulose II fractions of leaf CWMs (Table 3.2).

**Table 3.2.** Sugar composition in the pectin, hemicellulose I, and hemicellulose II fractions of cell walls in leaves of pBIN19- and hUGT1-transgenic tobacco plants

| Cell wall component | Monosaccharide | Mean ± standard deviation (%) | | | | |
|---|---|---|---|---|---|---|
| | | pBIN19 | *hUGT1*-2 | *hUGT1*-4 | *hUGT1*-14 | *hUGT1*-23 |
| Pectin | GlcA | 1.24 ± 0.54 | 1.32 ± 0.67 | 1.16 ± 0.56 | 1.25 ± 0.50 | 1.16 ± 0.39 |
| | GalA | 51.22 ± 9.80 | 46.40 ± 8.08 | 44.29 ± 3.68 | 49.44 ± 8.68 | 46.02 ± 9.81 |
| | Gal | 9.28 ± 1.74 | 11.95 ± 0.96 | 14.44 ± 2.94 [b] | 11.20 ± 0.80 | 13.42 ± 1.60 [a] |
| | Man | 1.84 ± 0.58 | 2.30 ± 0.71 | 2.92 ± 0.26 [b] | 1.83 ± 0.53 | 2.07 ± 0.83 |
| | Glc | 4.64 ± 2.10 | 5.05 ± 1.06 | 4.72 ± 0.71 | 6.03 ± 4.10 | 6.94 ± 3.68 |
| | Ara | 7.88 ± 1.22 | 7.82 ± 1.50 | 7.92 ± 0.83 | 7.65 ± 1.15 | 10.11 ± 1.79 [a] |
| | Xyl | 4.10 ± 1.69 | 5.65 ± 1.87 | 3.98 ± 1.01 | 3.36 ± 0.97 | 3.29 ± 1.69 |
| | Rha | 19.36 ± 4.49 | 19.50 ± 5.89 | 20.57 ± 4.16 | 19.25 ± 3.79 | 16.99 ± 3.69 |
| Hemicellulose I | GlcA | 6.90 ± 1.23 | 6.03 ± 0.56 | 7.38 ± 1.73 | 5.79 ± 0.58 | 6.42 ± 1.41 |
| | GalA | 12.50 ± 0.94 | 7.22 ± 0.40 | 8.16 ± 3.24 | 11.46 ± 4.14 | 11.26 ± 3.61 |
| | Gal | 7.80 ± 0.49 | 7.14 ± 0.74 | 8.61 ± 2.02 | 8.36 ± 1.31 | 8.72 ± 2.03 |
| | Man | 1.02 ± 0.08 | 1.41 ± 0.02 | 2.11 ± 0.97 | 1.41 ± 0.21 | 2.23 ± 1.86 |
| | Glc | 8.40 ± 0.78 | 17.49 ± 1.60 [b] | 14.90 ± 1.06 [b] | 13.13 ± 3.16 [a] | 13.94 ± 3.79 [a] |
| | Ara | 13.20 ± 0.27 | 8.63 ± 1.82 | 9.86 ± 3.95 | 10.12 ± 3.09 | 11.05 ± 3.06 |
| | Xyl | 45.84 ± 3.45 | 48.71 ± 6.29 | 44.79 ± 7.47 | 46.34 ± 9.77 | 42.62 ± 6.48 |
| | Fuc | 0.29 ± 0.07 | 0.07 ± 0.05 | 0.13 ± 0.12 | 0.23 ± 0.13 | 0.29 ± 0.20 |
| | Rha | 4.04 ±1.80 | 3.19 ± 1.60 | 4.05 ± 2.19 | 3.16 ± 2.41 | 3.49 ± 0.73 |
| Hemicellulose II | GlcA | 3.23 ± 0.68 | 1.99 ± 0.05 [a] | 2.53 ± 0.82 | 2.13 ± 0.19 [a] | 1.84 ± 0.09 [b] |
| | GalA | 8.90 ± 1.77 | 6.47 ± 2.71 | 5.39 ± 1.36 [a] | 6.28 ± 0.74 | 6.18 ± 1.52 |
| | Gal | 3.99 ± 0.49 | 5.34 ± 0.79 [a] | 6.02 ± 1.24 [b] | 6.25 ± 0.15 [b] | 8.54 ± 0.30 [b] |
| | Man | 1.39 ± 0.59 | 2.48 ± 2.15 | 1.86 ± 0.65 | 1.93 ± 0.53 | 2.59 ± 1.28 |
| | Glc | 24.05 ± 2.12 | 28.12 ± 2.04 | 28.49 ± 4.06 | 25.53 ± 2.14 | 27.08 ± 2.52 |
| | Ara | 8.98 ± 2.31 | 9.46 ± 1.41 | 8.32 ± 0.65 | 11.11 ± 1.57 | 10.84 ± 1.07 |
| | Xyl | 46.15 ± 3.18 | 43.33 ± 1.77 | 44.25 ± 1.69 | 44.11 ± 1.92 | 39.63 ± 1.94 [b] |
| | Fuc | tra | tra | tra | tra | tra |
| | Rha | 3.24 ± 0.63 | 2.71 ± 1.06 | 3.07 ± 0.52 | 2.60 ± 0.90 | 3.25 ± 1.06 |

[a]$P < 0.05$ and [b]$P < 0.01$

GlcA, D-glucuronic acid; GalA, D-galacturonic acid; Gal, D-galactose; Man, D-mannose; Glc, D-glucose; Ara, L-arabinose; Xyl, D-xylose; Fuc, L-fucose; and Rha, L-rhamnose. The percentage was calculated from the ratio of each monosaccharide to total monosaccharides. The mean and standard deviation of at least three repeated analysis from three independent samples were calculated.

### 3.3.2 Altered monosaccharide composition in stem cell wall polysaccharides of *hUGT1*-transgenic plants

Marked differences between leaf and stem CWMs were observed in the relative proportions of GalA and Xyl (Fig. 3.1B and 3.1C, Table 3.3). Compared with those in leaf CWMs, the proportion of GalA in stem CWMs was greatly decreased, whereas the proportion of Xyl was greatly increased, in both pBIN19-transgenic control and *hUGT1*-transgenic plants. These differences might be associated with the stem tissue composition, which contains a considerable amount of mature xylem and pith. The decrease in the GalA proportion was assumed to reflect the smaller proportion of pectic-polysaccharide-rich cells in the stem. A high amount of Xyl is derived from xylan in tobacco stems (58,59). Relatively unsubstituted xylans are abundant components of the secondary cell walls associated with the xylem (60). By contrast, little Glc was released from the stem CWMs because of cellulose crystallization in the secondary cell wall (Table 3.3). The GalA proportion in the *hUGT1*-transgenic plants tended to be reduced in comparison with that of the pBIN19-transgenic control. The proportions of the other monosaccharides were increased to some degree with little or no statistical significance (Table 3.3). The proportion of Gal in two transgenic lines (*hUGT1*-2 and -23) was significantly increased, but was not increased in two other lines (*hUGT1*-4 and -14) (Table 3.3). This difference among lines might be caused by differences in stem maturity during the cultivation period, because the plants of each transgenic-line were not completely homogeneous and showed some variation in growth rate.

The stem CWMs were divided into four fractions, namely pectin I (CDTA-soluble), pectin II ($Na_2CO_3$-soluble), hemicellulose I (1 M KOH-soluble), and hemicellulose II (4 M KOH-soluble) fractions. A marked difference in the monosaccharide composition between *hUGT1*-transgenic and pBIN19-transgenic control plants was observed in the pectin I fraction, which contains homogalacturonan, rhamnogalacturonan-I and -II, and type-II arabinogalactan (61). All *hUGT1*-transgenic lines showed remarkably higher Gal proportions compared with the pBIN19-transgenic control (Table 3.4). The Ara and Rha proportions in the *hUGT1*-transgenic lines were also higher.

**Table 3.3.** Monosaccharide composition of total cell wall polymers in stems of pBIN19- and *hUGT1*-transgenic tobacco plants

| Monosaccharide | Mean ± standard deviation (%) | | | | |
|---|---|---|---|---|---|
| | pBIN19 | *hUGT1*-2 | *hUGT1*-4 | *hUGT1*-14 | *hUGT1*-23 |
| GlcA | 7.67 ± 4.22 | 8.73 ± 3.56 | 7.65 ± 2.09 | 7.68 ± 3.48 | 9.05 ± 2.15 |
| GalA | 48.46 ± 5.18 | 35.75 ± 10.68 [a] | 38.87 ± 9.38 | 42.11 ± 7.76 | 38.33 ± 11.32 |
| Gal | 4.68 ± 0.38 | 7.16 ± 1.44 [b] | 4.12 ± 0.97 | 5.50 ± 1.05 | 6.28 ± 1.59 [a] |
| Man | 2.40 ± 0.68 | 3.76 ± 1.59 | 3.03 ± 1.14 | 3.10 ± 0.92 [a] | 3.37 ± 1.49 |
| Glc | 3.29 ± 1.15 | 5.58 ± 2.45 | 4.10 ± 2.17 | 4.69 ± 1.77 | 4.80 ± 2.56 |
| Ara | 2.00 ± 0.46 | 2.34 ± 1.32 | 2.05 ± 0.44 | 2.28 ± 0.57 | 2.21 ± 1.41 |
| Xyl | 29.01 ± 2.25 | 33.43 ± 3.08 [a] | 32.55 ± 3.69 | 31.46 ± 3.20 | 32.50 ± 1.32 |
| Fuc | tra | tra | tra | tra | tra |
| Rha | 2.50 ± 0.37 | 3.25 ± 0.93 | 2.82 ± 0.99 | 3.18 ± 0.85 | 3.46 ± 0.83 |

[a]$P < 0.05$ and [b]$P < 0.01$.

GlcA, D-glucuronic acid; GalA, D-galacturonic acid; Gal, D-galactose; Man, D-mannose; Glc, D-glucose; Ara, L-arabinose; Xyl, D-xylose; Fuc, L-fucose; and Rha, L-rhamnose. Values in parentheses are the ratio of each monosaccharide (%) to total monosaccharides without glucose. The mean and standard deviation of at least three repeated analyses from three independent samples were calculated.

These results suggested that an increased ratio of rhamnogalacturonan-I to homogalacturonan occurred in the *hUGT1*-transgenic plants.

In the pectin II fraction, compared with the pBIN19-transgenic control, the Ara proportion in *hUGT1*-transgenic lines was significantly lower, whereas the proportion of Xyl was higher. The richest monosaccharide was GalA, but considerable proportions of Gal, Ara, Xyl, and Rha were also observed, suggesting that this fraction contains homogalacturonan, rhamnogalacturonan-I, and xylogalacturonan, which seem to form a covalent linkage in each other (62,63). However, given that xylogalacturonan has not been identified previously in tobacco pectic-fraction components, the high Xyl proportion may be derived from xylan incorporated in homogalacturonan, which is abundant in the tobacco stem. Although xylan is isolated with the hemicellulose I fraction, some research suggests that syntheses of pectic polysaccharides and xylan are connected via a covalent linkage of the polymers or via synthesis in biosynthetic complexes (56).

In the hemicellulose I fraction, xylan and/or glucuronoxylan were indicated to predominate. The Gal proportion was not increased as in the leaf CWM. In the *hUGT1*-transgenic lines, Man proportions were slightly increased. A significant difference in Glc proportion between the pBIN19-transgenic control and the *hUGT1*-transgenic plants was observed, but because the proportion for line 4 was higher and those of the other lines were lower than that of the control, the variation in Glc proportion among the plant lines might be the result of a technical error during fractionation.

The proportions of most monosaccharides in the hemicellulose II fraction were altered. The *hUGT1*-transgenic lines showed a significant increase in Gal proportion. As in the leaf analysis, the Gal proportion in the *hUGT1*-transgenic lines 2 and 14 was twice that of the pBIN19-transgenic lines. Potential polysaccharide candidates containing Gal extracted in this fraction are xyloglucan and galactoglucomannan (64). Furthermore, the proportions of GlcA and Rha increased, whereas those of Man and Glc decreased. The decrease in the proportion of Man and Glc was suggestive of a decrease in glucomannan, which is the major hemicellulosic component of secondary cell walls.

Galactoglucomannan might be excluded as a candidate Gal acceptor in the hemicellulose II fraction, because galactoglucomannan and glucomannan have the same backbone structure (5).

### 3.3.3. OLIMP

In the cell wall monosaccharide analysis, the components of the pectin I and hemicellulose II fractions were candidates for hyper-galactosylation. Xyloglucan is a cell wall matrix polysaccharide involved in cross-linking adjacent cellulose microfibrils by hydrogen bonds, and was extracted in the hemicellulose II fraction by 4 M KOH. Xyloglucan comprises a backbone of (1→4)-β-D-Glc*p* residues substituted at *O*-6 with side chains of α-D-Xyl*p*. In dicotyledonous plants, such as tamarind and Arabidopsis, xyloglucan contains α-L-Fuc*p*-(1→2)-β-D-Gal*p* attached to the *O*-2 of some α-D-Xyl*p* residues, but in tobacco xyloglucan usually contains side chains of α-D-Xyl*p* and α-L-Ara*f*-(1→2)-α-D-Xyl*p*, forming arabinoxyloglucan, instead of α-L-Fuc*f*-(1→2)-β-D-Gal*p* (65). To assist with the description of xyloglucan structures, Fry et al. (66) developed an unambiguous nomenclature based on a one letter code according to substituents as follows: G, unsubstituted β-D-Glc*p*; X, α-D-Xyl*p*-(1→)-β-D-Glc*p*; S,X with α-L-Ara*f*-(1→2)-attached; L, X with β-D-Gal*p* (1→2)-attached. Therefore, tobacco xyloglucan usually includes few Gal residues. However, Sims et al. (67) analyzed a xyloglucan secreted from suspension-cultured cells of *Nicotiana plumbaginifolia* using xyloglucan-specific enzyme digestion followed by a mass spectrometric analysis, and detected the possible presence of Gal residues in the xyloglucan. Truelsen et al. (68) observed the presence of Gal in xyloglucan from the suspension-cultured cells and medium of *N. tabacum*. Thus, even though there is a possibility that the high proportion of Gal in the hemicellulose II fraction was from a hyper-galactosylated galactoglucomannan (64), I analyzed whether the xyloglucan of *hUGT1*-trangenic plants exhibited addition of Gal residues. The hemicellulose II fraction was digested with a xyloglucan-specific enzyme (xyloglucanase E-XEGP; 69) and released xyloglucan fragments were analyzed using MALDI-TOF-QIT-MS.

**Table 3.4.** Sugar composition in the pectin I, pectin II, hemicellulose I, and hemicellulose II fractions of cell walls in stems of pBIN19- and hUGT1-transgenic tobacco plants.

| Cell wall component | Monosaccharide | Mean ± standard deviation (%) | | | | |
|---|---|---|---|---|---|---|
| | | pBIN19 | *hUGT1*-2 | *hUGT1*-4 | *hUGT1*-14 | *hUGT1*-23 |
| Pectin I | GalA | 69.80 ± 6.25 | 36.06 ± 3.93 [b] | 45.68 ± 4.84 [b] | 44.70 ± 3.93 [b] | 42.56 ± 5.21 [b] |
| | Gal | 13.94 ± 3.14 | 37.72 ± 1.49 [b] | 29.64 ± 4.15 [b] | 30.85 ± 2.25 [b] | 32.09 ± 4.20 [b] |
| | Ara | 9.71 ± 2.48 | 15.75 ± 1.16 [b] | 17.33 ± 1.64 [b] | 13.49 ± 1.06 [a] | 14.66 ± 2.32 [b] |
| | Rha | 6.55 ± 0.98 | 10.48 ± 4.71 | 7.34 ± 0.88 | 10.96 ± 0.68 [a] | 10.70 ± 1.06 [a] |
| Pectin II | GalA | 38.42 ± 9.11 | 42.5 ± 2.95 | 35.56 ± 4.72 | 40.52 ± 2.24 | 35.27 ± 5.07 |
| | Gal | 24.04 ± 2.15 | 21.59 ± 1.63 | 22.29 ± 2.69 | 19.69 ± 0.56 | 23.79 ± 2.47 |
| | Ara | 14.11 ± 2.45 | 7.53 ± 0.45 [b] | 11.56 ± 0.29 [a] | 8.16 ± 0.22 [b] | 8.7 ± 0.65 [b] |
| | Xyl | 14.71 ± 2.08 | 23.04 ± 1.55 [b] | 21.68 ± 0.92 [b] | 26.3 ± 0.84 [b] | 23.89 ± 1.90 [b] |
| | Rha | 8.73 ± 2.54 | 5.34 ± 2.01 [a] | 8.91 ± 1.37 | 5.32 ± 1.41 [a] | 8.35 ± 0.35 |
| Hemicellulose I | GlcA | 14.83 ± 5.03 | 16.54 ± 3.07 | 15.00 ± 1.33 | 16.36 ± 1.03 | 14.63 ± 0.53 |
| | Gal | 0.92 ± 0.04 | 0.75 ± 0.14 | 1.20 ± 0.24 | 0.96 ± 0.05 | 0.98 ± 0.27 |
| | Man | 1.34 ± 0.10 | 2.24 ± 0.48 [b] | 1.90 ± 0.20 [a] | 2.01 ± 0.18 [a] | 1.30 ± 0.48 |
| | Glc | 5.48 ± 0.68 | 3.02 ± 0.53 [b] | 6.59 ± 0.55 [a] | 3.55 ± 0.45 [b] | 3.90 ± 0.31 [b] |
| | Ara | tra | 1.06 ± 0.15 | tra | 0.58 ± 0.36 | tra |
| | Xyl | 77.43 ± 4.26 | 76.37 ± 3.91 | 75.31 ± 1.73 | 75.04 ± 1.25 | 79.21 ± 0.55 |
| Hemicellulose II | GlcA | 8.91 ± 5.15 | 13.23 ± 0.50 | 9.98 ± 2.90 | 11.51 ± 0.57 | 11.55 ± 1.18 |
| | Gal | 10.66 ± 0.80 | 21.23 ± 0.32 [b] | 12.25 ± 0.37 [b] | 19.13 ± 0.84 [b] | 10.28 ± 0.33 |
| | Man | 14.45 ± 0.89 | 6.53 ± 0.55 [b] | 13.17 ± 2.55 | 7.23 ± 0.61 [b] | 6.56 ± 1.50 [b] |
| | Glc | 11.27 ± 7.27 | 3.76 ± 0.08 [a] | 7.08 ± 1.53 | 4.89 ± 0.44 [a] | 4.59 ± 0.87 [a] |
| | Ara | 7.62 ± 0.16 | 7.43 ± 0.03 | 6.64 ± 0.20 [b] | 8.33 ± 0.23 [b] | 4.82 ± 0.09 [b] |
| | Xyl | 45.7 ± 3.58 | 41.62 ± 0.21 | 45.91 ± 3.06 | 43.74 ± 3.13 | 58.36 ± 3.25 [b] |
| | Rha | 3.93 ± 1.34 | 5.77 ± 0.13 | 4.98 ± 1.20 | 5.18 ± 1.62 | 3.83 ± 1.20 |

[a] $P < 0.05$, [b] $P < 0.01$

GlcA, D-glucuronic acid; GalA, D-galacturonic acid; Gal, D-galactose; Man, D-mannose; Glc, D-glucose; Ara, L-arabinose; Xyl, D-xylose; and Rha, L-rhamnose. The percentage was calculated from the ratio of each monosaccharide to total monosaccharides. The mean and standard deviation of at least three repeated analysis from three independent samples were calculated.

Tamarind xyloglucan was used as a standard. The tamarind xyloglucan digest showed a simple mass profile with peaks at 1085, 1247, and 1409 (m/z) corresponding to $Hex_4Pent_3$ (meaning 4 hexose and 3 pentose, XXXG), $Hex_5Pent_3$ (XLXG/XXLG), and $Hex_6Pent_3$ (XLLG), respectively (Fig. 3.2A), as reported previously (69). However, the peak at 1085 (m/z) was small, and additional peaks at 953 and 1115 (m/z) corresponding to $Hex_4Pent_2$ (XXGG/GXXG) and $Hex_5Pent_2$ (GLXG/XLGG/GXLG/XGLG), respectively, were also detected. These results may be attributable to the MALDI-TOF-QIT-MS detection properties. This instrument equips a reflectron with a long flight path and an ion trap. Monosaccharides with comparably weaker linkages in oligosaccharides are partially lost by fragmentation during the long flight and ion trapping prior to the reflectron analyzer, so called "in-source decay" (70). Consequently, it is likely that the additional peaks at 953 and 1115 (m/z) were derived from partial xylose-desorption from xyloglucan oligosaccharides corresponding to 1085 and 1247 (m/z), respectively, because each of the former m/z values were determined after subtracting 132 corresponding to anhydroxylose from each of the latter m/z values. Indeed, post-source decay (PSD) fragmentation analysis of xyloglucan oligosaccharides by MALDI-TOF-MS, which provides sequential information as glycosidic linkage cleaving, demonstrated that $Hex_5Pent_2$ GXLG and XGLG were possible xylose-deficient oligosaccharides derived from $Hex_5Pent_3$ XXLG (71). Therefore, the additional peaks at 953 and 1115 (m/z) must have represented XXGG/GXXG and GLXG/XLGG/GXLG/XGLG, respectively.

The mass profile from the digested hemicellulose II fraction of tobacco leaves differed from that of tamarind. Given that the main peaks of the digested oligosaccharides in the mass profile were 923, 953, 1085, 1115, 1217, 1247, 1380, and 1409 (m/z), which were similar to those of *N. plumbaginifolia* (67), the mass profile of *N. tabacum* was comparable to that of *N. plumbaginifolia* (Fig. 3.2B and 3.2C). These selected peaks corresponded to xyloglucan oligosaccharides without *O*-acetylation. In addition to the selected peaks, many other peaks were detected, of which some were higher than those of the selected peaks. Similar mass profiles have been reported in a previous OLIMP analysis of tobacco xyloglucan oligosaccharides digested with the same xyloglucan-specific enzyme, E-XEGP (55). Since m/z values of some peaks, for

example 834 and 997 (m/z) whose heights were larger than most of the selected peaks, were near to those of *O*-acetylated xyloglucan oligosaccharides of *N. plumbaginifolia*, these peaks might represent *O*-acetylated oligosaccharides. However, in the present hemicellulose II extraction, the polysaccharides were deacetylated by 4 M KOH; therefore, these peaks cannot be *O*-acetylated oligosaccharides. Alternatively, some of these additional peaks might derive from desorption of xyloglucan oligosaccharides by "in-source decay", which is one of the properties of MALDI-TOF-QIT-MS as described above. Although such additional peaks should be included in an analysis, they were not considered here to avoid confusion. Therefore, my present analysis only targeted non-*O*-acetylated peaks because my purpose was to estimate hyper-galactosylation of selected peaks that had already been identified.

In particular, a large peak at 1380 m/z, corresponding to SSGGG, appeared in the digest of *N. tabacum*, which was rarely seen in the digest of tamarind (Fig. 3.2A, 3.2B, and 3.2C). On the basis of the mass profile of *N. plumbaginifolia*, the peaks at 1247 (m/z) seemed to represent SXGGG/XSGGG or XLXG/XXLG and the peak at 1409 (m/z) seemed to represent XLLG, which contain Gal. The peak at 1115 m/z seemed to be $Hex_5Pent_2$, representing XXGGG, but it might also represent XLGG, which was not detected in *N. plumbaginifolia*. While the peaks at 1115, 1247, and 1409 (m/z) were detected in both pBIN19- and *hUGT1*-transgenic plants, these ion intensities (% area) of the *hUGT1*-transgenic lines were high compared with those of the pBIN19-transgenic control line (Fig. 3.2B and 3.2C, Table 3.5). Although MALDI-TOF-MS is used more frequently for qualitative analysis of molecules than quantitative estimations, the ion intensity (% area) is correlated to the abundance of the oligosaccharides (72). This OLIMP result suggested that the xyloglucan of *hUGT1*-transgenic plants was hyper-galactosylated. A more detailed analysis of the XLLG peak using MS/MS is currently underway.

I hypothesized that enhanced UDP-Gal transport to the Golgi apparatus by hUGT1 contributes to averting the toxicity of Gal contained in the culture medium, resulting in increased tolerance to Gal.

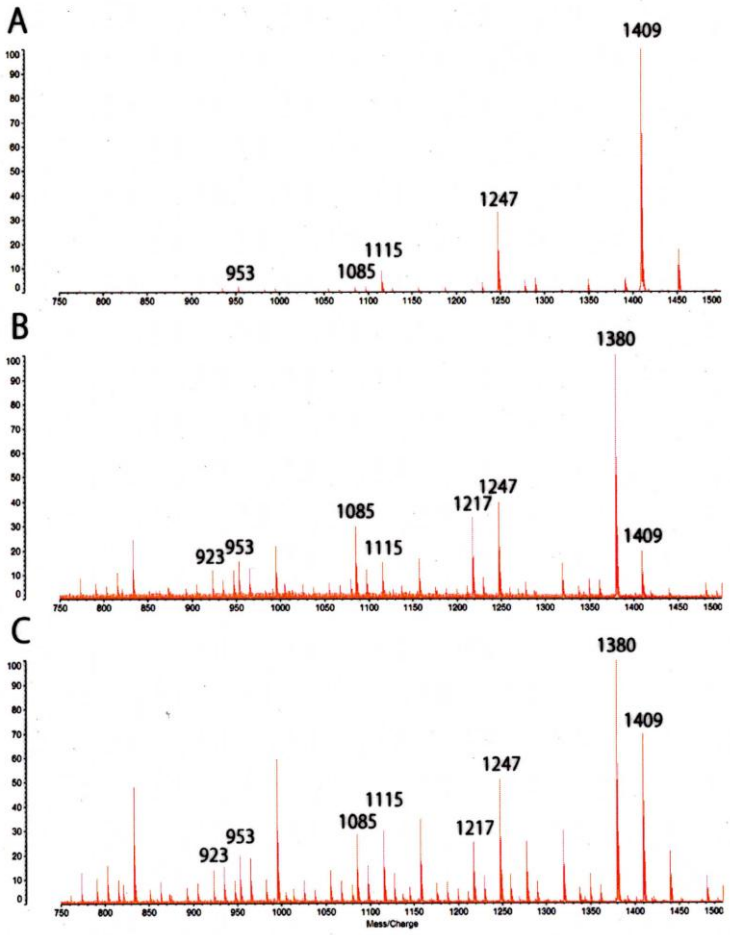


**Fig. 3.2.** OLIMP analysis of pBIN- and *hUGT1*-transgenic tobacco xyloglucan. Xyloglucan contained in the hemicellulose II fraction isolated from leaves was digested with E-XEGP, and the released oligosaccharides were analyzed using MALDI-TOF-QIT-MS. (A) Mass profile of tamarind xyloglucan as an enzyme digestion standard. (B) Mass profile of pBIN19-transgenic tobacco plants as a control. (C) Mass profile of *hUGT1*-transgenic tobacco plant line 23. Numbers indicate the m/z values of each peak. Numbers on the left side of the *y*-axis indicate percentage of mass peaks.

**Table 3.5.** Comparison of ion intensity (% area) of oligosaccharides obtained from the leaf hemicellulose II fraction of pBIN19- and *hUGT1*-transformed tobacco plants

| Transgenic line | | Oligosaccharide | | | | | | | |
|---|---|---|---|---|---|---|---|---|---|
| Pseudomolecular ion $[M+Na]^+$(m/z) | | 923 | 953 | 1085 | 1115 | 1217 | 1247 | 1380 | 1409 |
| Composition | | $Hex_3Pent_3$ | $Hex_4Pent_2$ | $Hex_4Pent_3$ | $Hex_5Pent_2$ | $Hex_4Pent_4$ | $Hex_5Pent_3$ | $Hex_5Pent_4$ | $Hex_6Pent_3$ |
| Glycosyl structure | | SXG<br>XSG | XXGG | SXGG<br>XSGG | XXGGG<br>GLXG<br>XLGG<br>GXLG<br>XGLG | SSGG | SXGGG<br>XSGGG<br>XLXG<br>XXLG | SSGGG | XLLG |
| Ion intensity (% area) | pBIN19 | 8.97 | 12.73 | 22.54 | 13.67 | 30.6 | 39.44 | 100 | 17.78 |
| | *hUGT1*-2 | 12.94 | 13.04 | 23.12 | 20.31 | 30.65 | 55 | 100 | 64.22 |
| | *hUGT1*-4 | 15.11 | 20.26 | 30.08 | 33.59 | 25.31 | 53.33 | 100 | 63.96 |
| | *hUGT1*-14 | 27.58 | 26.96 | 44.75 | 35.17 | 33.6 | 57.55 | 100 | 55.74 |
| | *hUGT1*-23 | 9.94 | 14.23 | 22.54 | 24.2 | 22.07 | 46.17 | 100 | 70.81 |

Leaf hemicellulose II fractions were digested with E-XEG, and released oligosaccharides were analyzed with MALDI-TOF-QIT-MS. An unambiguous nomenclature with the letters: G, unsubstituted b-D-Glcp; X, a-D-Xylp-(1/6)-b-D-Glcp; S, X with a-L-Araf-(1 /2)-attached and L, X with b-D-Galp (1/2)-attached. Hex, hexose; Pent, pentose.

To examine whether the *hUGT1*-transgenic plants exhibited increased Gal tolerance, the *hUGT1*- and pBIN19-transgenic plants were cultured on MS medium containing 0 to 0.6% Gal. Figure 3 shows representative results from one of the Gal tolerance assays. Similar results were obtained in the other two tests (data not shown). The influence of Gal on pBIN19-transgenic plants was apparent at 0.2% Gal. The growth of aerial parts was weakly suppressed at 0.3% Gal (Fig. 3.3A), strongly suppressed at 0.4% Gal, and completely inhibited at Gal concentrations of 0.5% or higher (data not shown). Roots were more sensitive to Gal. At 0.2% Gal, the root tips of pBIN19-transgenic plants turned brown and root elongation was suppressed by ~50%. The suppression of root elongation was completely inhibited at 0.4% Gal (Fig. 3.3B). However, the *hUGT1*-transgenic plants were tolerant to Gal. The aerial parts were not suppressed at 0.3% Gal (Fig. 3.3A), weakly suppressed at 0.4% Gal, strongly suppressed at 0.5% Gal, and almost entirely inhibited at 0.6% Gal (data not shown), and displayed the same responses as those of pBIN19-transgenic plants grown at each 0.1%-low level of the Gal concentrations. The roots also showed increased Gal tolerance but root elongation was largely inhibited at 0.5% Gal (Fig. 3.3B). Moreover, when *hUGT1*-transgenic plants grew at 0.3% Gal, their root lengths resembled those of *pBIN19*-transgenic plants grown at 0.2%, while *hUGT1*-transgenics at 0.4% resembled *pBIN19*-trangenics grown at 0.3% Gal (Fig. 3.3B). I hypothesized that the Gal tolerance of *hUGT1*-transgenic plants was caused by enhanced UDP-Gal Golgi transport activity. To determine whether Gal in the culture medium was transported to the Golgi apparatus as a substrate for Gal-containing cell wall matrix polysaccharide, CWMs from leaves of plants cultured on Gal-containing media were isolated to measure the relative proportion of monosaccharides. On medium lacking Gal, the monosaccharide compositions of the transgenic plants were similar to those of the leaves of plants grown in soil (Table 3.6). However, the relative proportions of each monosaccharide in the *in vitro* cultured plants were different from those of the soil-grown plants. In the in *vitro* cultured plants, the proportions of Gal and Ara were higher, whereas those of GlcA and Xyl were lower, compared with those of soil-grown plants. The proportions of Gal in the CWMs of the *hUGT1*-transgenic plant lines cultured on 0% Gal medium were higher than those of the pBIN19-transgenic control, as observed for plants grown in soil.

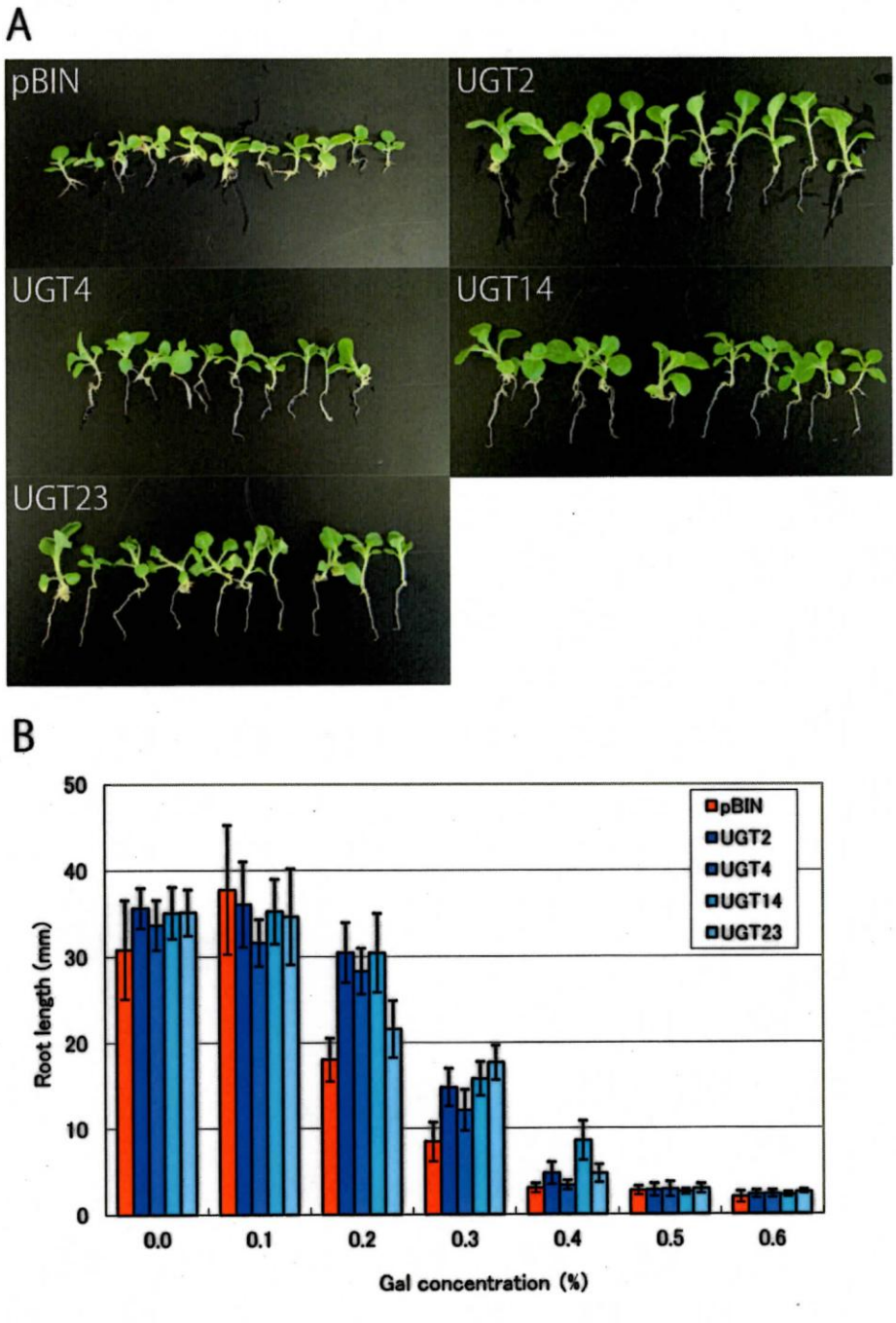


**Fig. 3.3.** Galactose (Gal) tolerance of pBIN- and *hUGT1*-transgenic tobacco plants. (A) Seedlings grown on Murashige and Skoog solid medium containing 0.3% D-Gal. White scale bars: 1 cm. (B) Root length of pBIN- and *hUGT1*-transgenic plants grown on Murashige and Skoog solid medium supplemented with various concentrations of Gal. The error bar represents the standard deviation. pBIN, pBIN19-transgenic control plants; UGT2, -4, -14 and -23, *hUGT1*-transgenic lines. Statistical significance: *, $P<0.05$; **, $P<0.01$.

**Table 3.6.** Monosaccharide composition of total cell wall polymers in pBIN19- and *hUGT1*-transgenic tobacco plants cultured in the presence of 0, 0.2, and 0.3% galactose

| Gal concentration | Monosaccharide | Mean ± standard deviation (%) | | | | |
|---|---|---|---|---|---|---|
| | | pBIN19 | *hUGT1*-2 | *hUGT1*-4 | *hUGT1*-14 | *hUGT1*-23 |
| 0% | GlcA | 1.79 ± 0.26 | 1.65 ± 0.25 | 1.57 ± 0.17 | 1.41 ± 0.24 | 1.44 ± 0.20 |
| | GalA | 75.98 ± 4.45 | 71.09 ± 2.06 | 71.59 ± 3.63 | 73.03 ± 3.02 | 71.55 ± 2.05 |
| | Gal | 7.64 ± 1.74 | 11.07 ± 1.44 [a] | 11.15 ± 1.60 [a] | 9.52 ± 1.46 | 9.62 ± 1.13 |
| | Man | 1.04 ± 0.20 | 1.46 ± 0.30 [a] | 1.28 ± 0.21 | 1.26 ± 0.22 | 1.23 ± 0.15 |
| | Glc | 1.98 ± 0.45 | 2.41 ± 0.45 | 2.61 ± 1.18 | 2.53 ± 0.33 | 4.06 ± 0.47 [b] |
| | Ara | 3.23 ± 0.55 | 3.53 ± 0.24 | 3.74 ± 0.23 | 3.47 ± 0.30 | 3.59 ± 0.38 |
| | Xyl | 4.96 ± 0.30 | 4.06 ± 1.11 | 4.33 ± 0.76 | 4.38 ± 0.48 | 3.59 ± 0.38 |
| | Rha | 3.39 ± 1.00 | 4.73 ± 1.16 | 3.73 ± 0.99 | 4.40 ± 1.13 | 4.21 ± 0.87 |
| 0.2% | GlcA | 1.19 ± 0.13 | 1.34 ± 0.20 | 1.52 ± 0.14 [a] | 1.38 ± 0.02 | 1.59 ± 0.19 [b] |
| | GalA | 76.88 ± 3.89 | 72.75 ± 2.25 | 69.61 ± 2.91 [a] | 74.11 ± 4.09 | 70.56 ± 2.77 [a] |
| | Gal | 8.14 ± 1.41 | 10.53 ± 1.33 [a] | 11.69 ± 1.15 [b] | 8.72 ± 1.27 | 9.92 ± 1.01 |
| | Man | 1.09 ± 0.21 | 1.33 ± 0.19 | 1.40 ± 0.13 | 1.21 ± 0.20 | 1.46 ± 0.22 |
| | Glc | 2.04 ± 0.54 | 2.31 ± 0.38 | 2.41 ± 0.26 | 1.92 ± 0.28 | 2.81 ± 0.75 |
| | Ara | 3.29 ± 0.55 | 3.50 ± 0.08 | 3.85 ± 0.45 | 3.74 ± 0.56 | 4.02 ± 0.38 |
| | Xyl | 3.82 ± 0.41 | 3.71 ± 0.69 | 4.89 ± 1.03 | 4.91 ± 0.61 | 4.80 ± 0.41 |
| | Rha | 3.55 ± 0.93 | 4.54 ± 0.86 | 4.63 ± 0.75 | 4.01 ± 1.16 | 4.84 ± 0.97 |
| 0.3% | GlcA | 1.15 ± 0.07 | 1.44 ± 0.44 | 1.47 ± 0.61 | 1.75 ± 0.57 | 1.59 ± 0.39 |
| | GalA | 78.20 ± 1.25 | 75.52 ± 5.26 | 72.38 ± 5.14 | 69.90 ± 3.88 [a] | 69.44 ± 3.39 [a] |
| | Gal | 8.23 ± 0.17 | 10.55 ± 1.93 | 10.41 ± 2.10 | 11.61 ± 1.70 [a] | 10.28 ± 0.33 [a] |
| | Man | 0.96 ± 0.04 | 1.34 ± 0.30 | 1.39 ± 0.35 | 1.54 ± 0.34 [a] | 1.58 ± 0.28 [a] |
| | Glc | 1.53 ± 0.01 | 2.08 ± 0.45 | 2.37 ± 0.58 [a] | 2.19 ± 0.53 | 2.36 ± 0.33 [a] |
| | Ara | 2.99 ± 0.22 | 3.54 ± 0.53 | 3.41 ± 0.57 | 3.72 ± 0.28 | 3.82 ± 0.35 [a] |
| | Xyl | 3.92 ± 0.36 | 4.59 ± 0.37 | 4.57 ± 0.30 | 4.48 ± 0.68 | 4.75 ± 0.31 [a] |
| | Rha | 3.02 ± 0.49 | 3.94 ± 1.56 | 3.99 ± 0.96 | 4.81 ± 1.02 | 4.30 ± 0.73 |

[a] $P < 0.05$, [b] $P < 0.01$

GlcA, D-glucuronic acid; GalA, D-galacturonic acid; Gal, D-galactose; Man, D-mannose; Glc, D-glucose; Ara, L-arabinose; Xyl, D-xylose; and Rha, L-rhamnose. The percentage was calculated from the ratio of each monosaccharide to total monosaccharides. The mean and standard deviation of at least three repeated analysis from three independent samples were calculated.

However, the relative Gal proportions in *hUGT1*- and pBIN19-transgenic plants did not vary among the 0%, 0.2%, and 0.3% Gal-containing media. The increased Gal proportion in the *hUGT1*-transgenic plants was consistent at the three Gal concentrations. These results suggested that the increased Gal tolerance of *hUGT1*-transgenic plants was caused by increased UDP-Gal transport activities. However, hUGT1 activity seemed not to increase with increasing Gal concentrations in the culture medium.

### 3.4. Discussion

Nucleotide sugars in the Golgi apparatus are used as substrates in the production of complex sugar chains on glycoproteins. In addition, in plant cells, nucleotide sugars are also used as substrates in the production of non-cellulosic polymers, such as hemicellulosic and pectic polysaccharides. Therefore, the NSTs located in the membrane of the Golgi apparatus are indispensable for the transport of specific nucleotide sugars from the cytosol to the Golgi lumen, where they are used to produce carbohydrates that become components of the plant cell walls. An UDP-Glc transporter functions to supply UDP-glucose as a partner of the glucosyltransferase responsible for the incorporation of Glc into Glc-containing polysaccharides, which indicates the possible role of NSTs in polysaccharide biosynthesis in plant cells (76). However, although recent studies have revealed the functions of plant NSTs (31,33–35,77–80), few important details about the relationship between the transport of nucleotide sugars and the production of cell wall polymers were discerned.

Khalil et al., introduced the human UDP-Gal transporter *hUGT1*, for which the function is well characterized among previously reported UDP-Gal transporters, into tobacco plant cells (13). I examined whether excessive transport of UDP-Gal affects the monosaccharide composition of non-cellulosic cell wall polymers. The results clearly indicated that overexpression of *hUGT1* caused hyper-galactosylation of CWMs in the *hUGT1*-transgenic tobacco plants (Tables 3.1 and 3.3). The increase in the relative Gal proportion in leaf and stem CWMs (the highest increases were 2.76- and 1.55-fold, respectively) suggested that the enhanced UDP-Gal transporter activity was enough to "hyper-galactosylate" plant cell walls. The hyper-galactosylated polysaccharides were the pectin and hemicellulose II fractions in the leaves (Table 3.2), and pectin I and hemicellulose II fractions in the stems. Pectic polysaccharides usually consist of homogalacturonan, and rhamnogalacturonan-I and -II, which are rich in GalA. Other major monosaccharides present in pectic polysaccharides are Rha, Gal, and Ara (40). Although Gal was not the only elevated monosaccharide, the relative Gal proportion in the pectin fraction was increased. It is presumed that Gal is mainly incorporated in pectic galactan and the type-I arabinogalactan side chains as a component of

rhamnogalacturonan-I, which are the most likely Gal acceptors. However, because the stem pectin II fraction, which showed a high proportion of Gal, was indicated to contain rhamnogalacturonan-I, determination of the acceptors of excessive Gal is required in future work. Rhamnogalacturonan-II is also a potential candidate Gal acceptor. However, considering the low Gal allocation in its considerably conserved structure and the lower proportion in pectin (~10%; 56), additional Gal acceptance seemed to be limited. By contrast, type-II arabinogalactan is likely to have been hyper-galactosylated because an increased Gal proportion in the sugar moiety of the arabinogalactan protein was demonstrated in our previous report (13).

A similar hyper-galactosylation was observed in the hemicellulose II fraction, which contains xyloglucan and galactoglucomannan. In contrast to that in Arabidopsis and tamarind, tobacco xyloglucan usually contains Glc and Xyl as the main structural materials, and Ara instead of Gal and Fuc, giving it the name arabinoxyloglucan (65). Therefore, additional Gal incorporation in the hemicellulose II fraction might be limited to only galactoglucomannan. Alternatively, being a pectic polysaccharide, rhamnogalacturonan-I, which tightly binds to hemicellulosic components (57), may be a Gal-acceptor polysaccharide in the hemicellulose II fraction. However, Truelsen et al. (68) indicated the possible presence of Gal in the xyloglucan of *N. tabacum*. The mass detection of xyloglucan oligosaccharides released by xyloglucan-specific enzyme digestion strongly suggests the presence of Gal in the xyloglucan of *N. plumbaginifolia* (68) and *N. tabacum* (55). I performed a xyloglucan oligosaccharide analysis of *hUGT1*-transgenic plants digested by xyloglucan-specific enzymes using MALDI-TOF-MS (53). The OLIMP analysis revealed a mass peak at 1115, 1247, and 1409 (m/z), the possible Gal-containing xyloglucan fragments GLXG/XLGG/GXLG/XGLG, XLXG/XXLG, and XLLG, respectively, which were released from the hemicellulose II fraction of tobacco leaves (Fig. 3.2A and B, Table 3.5). When the highest peak area of xyloglucan at 1380 m/z, corresponding to SSGGG, was used as a peak standard, the peak areas at 1115, 1247, and 1409 (m/z) in the *hUGT1*-transgenic plant lines increased compared with those of the pBIN19-transgenic control (Fig. 3.2C, Table 3.5). This result suggested that xyloglucan is an acceptor of Gal in the hemicellulose II fraction. It is interesting that the intrinsically low

Gal-containing tobacco xyloglucan is hyper-galactosylated by excess UDP-Gal in the Golgi lumen. Gal residues of xyloglucan function in the maintenance of the mechanical strength of primary cell walls (22). An increased Gal content in xyloglucan might increase the tensile strength of the cell wall. Tests to determine whether the *hUGT1*-transgenic plants show altered strength are in progress.

The *hUGT1*-transgenic plants exhibited increased Gal tolerance. Increased Gal tolerance in transgenic plants has been reported previously. Overexpression of UDP-glucose epimerase (UGE) in potato induces strong Gal tolerance (46). Overexpression of galactosyltransferase (GalT) in *Arabidopsis* also confers remarkable Gal tolerance (47). However, because Gal tolerance conferred by a UDP-Gal transporter gene has not been reported previously, the present study is the first report that enhanced UDP-Gal transport activity in the Golgi apparatus may increase Gal-tolerance capability. The enhanced stream of Gal from the cytosol to the cell wall via the Golgi apparatus contributes to increased Gal tolerance. This result also demonstrates the enhanced Gal-transport activity in *hUGT1*-transgenic tobacco plants. At toxic concentrations Gal inhibits plant cell proliferation. However, increased Gal content in the CWMs of *hUGT1*-transgenic tobacco plants under high Gal concentrations was observed, which resulted in growth suppression in control plants. At 0.2%, 0.3%, and 0.4% Gal, the growth of aerial parts and roots of *hUGT1*-transgenic plants was almost identical to that of pBIN19-transgenic plants grown at each 0.1%-low concentration of Gal, thus the increased Gal tolerance appeared to result from the additional UDP-Gal transport activity caused by *hUGT1* expression. To enhance Gal tolerance, supplementary activity of UDP-Gal pyrophosphorylase (also known as UDP-glucose:galactose-1-phosphate uridyltransferase), which is responsible for the conversion of Gal-1-phosphate to UDP-Gal, might also be required (81). Joersbo et al. (2003) reported that Gal-1-phosphate toxicity could be eliminated by expression of *E. coli* UDP-Gal pyrophosphorylase in potato (82).

Enhanced Gal transport to the Golgi apparatus by *hUGT1* expression gave rise not only to increased content of Gal in Gal-containing polysaccharides, but also to a dynamic change in cell wall polymer composition. The significant decrease in GalA

proportion in the pectin fraction suggested that an increased ratio of rhamnogalacturonan-I to homogalacturonan (Tables 3.1–3.4); the tobacco-specific arabinoxyloglucan, which usually lacks Gal, was also hyper-galactosylated (Table 3.5), and increased callose biosynthesis was hypothesized. Although callose is not a cell wall matrix polysaccharide, this polymer can be extracted by 1 M NaOH (83) and its presence in tobacco leaves has been demonstrated by anti-callose antibody staining (55). However, the reason why callose deposition was increased in the *hUGT1*-transgenic plants is unknown. There are many examples of callose synthesis in response to injury, cold, heavy metals accumulation, and attack by various pathogens. If, in the *hUGT1*-transgenic plants, the hyper-galactosylation of cell wall matrix polysaccharides mimics some stress conditions (84), it is likely that increased callose deposition arises, resulting in the increased proportion of Glc in the hemicellulose I fraction. Elucidation of the relationship between callose deposition and galactosylation level of cell wall matrix polysaccharides is required in the future. These phenomena may suggest plasticity in cell wall biosynthesis.

Other studies have reported an increased Gal content in the cell walls of transgenic plants (46). Among the Gal-containing polysaccharides in the cell wall, some serve not only architectural functions but also show signal transduction activities (40). Oligosaccharides derived from xyloglucan show biological activities, such as the inhibition of 2,4-D-stimulated growth (41) or promotion of growth (42). Oligosaccharides derived from galactoglucomannan, one of the hemicellulosic polymers, also show an inhibitive effect on 2-4-D-induced cell elongation (43), cause an increase in cell population density, and alter the protoxylem/metaxylem tracheary element ratio (44). Thus, changes in Gal-containing cell wall polysaccharides might have a strong impact on plant growth and development. These results may indicate a novel plant modification strategy that may be useful for crop improvement in the future.

In conclusion, I demonstrated that *hUGT1* expression in tobacco plants caused hyper-galactosylation of cell wall matrix polysaccharides, dynamic changes in cell wall polymer composition, and increased Gal tolerance. To understand the relationship among Gal content in cell wall matrix polysaccharides, cell wall dynamics and the plant

phenotype,establishment of a regulatable modification method for hyper-galactosylation of cell wall components by combinatorial expression of the genes for exogenous UDP-galactose epimerase, hUGT1, and galactosyltransferase is currently in progress.

# Chapter 4. Expression of the human UDP-galactose transporter gene hUGT1 in tobacco plants enhanced plant hardness

## 4.1. Introduction

The cell wall is the principal structural element responsible for plant forms. The deposition and modification of cell wall materials play essential roles not only in plant growth, development and support but also in plant responses to environmental and pathogen-induced stresses (26). Most photosynthetically fixed carbon is incorporated into polymers that construct plant cell walls, which are the most abundant renewable resource on earth. Furthermore, cell wall materials are vital dietary components for animals, including humans, because they are sources of nutrients. Additionally, they are of practical importance for humans as sources of natural fibers for textiles and paper products. Thus, the increased production of cell wall polymers in a plant body has the advantages of reducing $CO_2$ emissions, as well as accumulating a renewable resource that can be used for food and industrial purposes.

Plants have two types of cell walls. Primary cell walls are synthesized during cell growth and consist mainly of polysaccharides that can be broadly classified as cellulose, cellulose-binding hemicelluloses and pectins. The primary cell walls provide mechanical stability with sufficient extensibility to permit cell expansion during cell growth. Cellulose is synthesized at the plasma membrane in the form of paracrystalline microfibrils, whereas hemicelluloses and pectins are synthesized within Golgi cisternae as matrix polysaccharides (27,15). Secondary cell walls, which are composed of cellulose, hemicellulose and lignin, are deposited between the primary cell wall and the plasma membrane at specialized cell types, such as xylem elements and sclerenchyma cells. They are produced after the cessation of cell growth and confer mechanical stability to the plant body, so it can stand against gravitational forces (27).

In plant cells, as in animal cells, glycoproteins and glycolipids are synthesized in the Golgi apparatus. In addition, cell wall matrix polysaccharides, such as hemicellulose

and pectin, are biosynthesized in the Golgi apparatus (27,15). To produce the matrix polysaccharides, glycosyltransferases carry out sequential additions of sugar residues in the Golgi apparatus (28). To biosynthesize matrix polysaccharides, nucleotide sugar transporters (NSTs) are indispensable for the translocation of substrates into the lumen of the Golgi apparatus and act as partners of the glycosyltransferases (14). Genes that encode proteins in the NST family have been isolated from animal, plant and yeast cells (29). UDP-galactose transporters are NST family members and are involved in the transport of UDP-galactose into the Golgi lumen (29). UDP-galactose transporters have been described in humans, rodents, *Drosophila*, *Caenorhabditis elegans*, *Entamoeba*, *Giardia*, *Leishmania*, yeast (30), *Arabidopsis* (12) and rice (*Oryza sativa*) (31). Consequently, as in animal cells, plant NSTs must play crucial roles in the import of nucleotide sugars into the Golgi apparatus. The *Arabidopsis* UDP-galactose/UDP-glucose transporters AtUTr1 (32), AtUTr2 (33), AtUDP-GalT1, AtUDP-GalT2 (34) and AtNST-KT1 (35) have been identified. Furthermore, three UDP-galactose transporters, OsUGT1, 2 and 3, have been isolated from rice (31).

Khalil et al., previously reported on the characteristics of tobacco plants transformed with the human UDP-galactose transporter 1 gene (*hUGT1*; 38), designated *hUGT1*-transgenic tobacco plants (13). hUGT1 is the first known mammalian nucleotide sugar transporter, and its structure and functions have been elucidated (38,85). Although a number of plant UGTs have been identified (12,31-35), we chose hUGT1, as the best-studied UGT, for our investigations. The hUGT1 expressed in tobacco plants was mainly localized to the trans-Golgi network and endoplasmic reticulum in tobacco cells, and it showed a UDP-galactose transporter activity, as in human cells (85). These *hUGT1*-trasgenic plants displayed enhanced growth during cultivation in soil.

Furthermore, I indicated in the previous chapter that the enhanced UDP-galactose transport activity resulting from the expression of *hUGT1* altered the monosaccharide compositions of cell wall matrix components in the *hUGT1*-transgenic plants. There was an increase in the ratio of galactose to total monosaccharide residues in the *hUGT1*-transgenic plants (86), and the increased galactose ratio, so called

hyper-galactosylation, was observed for xyloglucan in hemicellulose, rhamnogalacturonan I in pectin (86) and the arabinogalactan proteins (13). This increase in the galactose ratio was caused by an excess galactose transport activity from cytoplasm to Golgi lumen. This hyper-galactosylation of cell wall matrix polymers appeared to increase not only alterations in the cell wall structure but also the perception of environmental signals, such as phytohormones.

The *hUGT1*-transgenic plants were harder and more rigid to the touch than the pBIN19-transgenic plants. Increases in leaf thickness, caused by an enhanced amount of spongy tissue, greater numbers of xylem vessels in the stem, and an increased accumulation of lignin, were observed in the *hUGT1*-transgenic plants (13). Furthermore, the hyper-galactosylation of xyloglucan, which is a hemicellulose polysaccharide, was also presumed to enhance the hardness of *hUGT1*-transgenic tobacco (22). However, this hardness might result not only from these characteristics of *hUGT1*-transgenic plants but from other unknown reasons as well. Here, the practical hardness of *hUGT1*-transgenic plants was confirmed by physical strength measurements of leaves and stems using a tensile tester. Next, I determined whether the cell wall thickness in *hUGT1*-transgenic plants was altered. Finally, I demonstrated that the *hUGT1*-transgenic plants displayed an increased accumulation of cell wall materials, resulting in an increased biomass. The contribution of the heterologous expression of *hUGT1* to the increased accumulation of cell wall materials is discussed.

## 4.2. Materials and methods

### 4.2.1. Plant materials and growth conditions

Tobacco plants (*Nicotiana tabacum* cv. SR-1) containing *hUGT1* (38) driven by the CaMV 35S promoter (pBIN-hUGT1) and the empty vector pBIN19 were used as *hUGT1*-transgenic plants and control pBIN19-transgenic plants, respectively, as described previously (13). T1 plants of each line were transplanted into soil in pots for cultivation. To compare these transgenic plants, wild type tobacco plants without any transgenes were also used. These plants were cultured *in vitro* for 1 month, transferred to soil in pots and cultivated with the addition of 1:1,000 diluted Hyponex fertilizer (Hyponex Japan, Osaka, Japan) at 25°C with a 16-h photoperiod under a fluorescent daylight lamp (50 μmol/$m^2$/s) in a climate-controlled room. The leaves and stems of plants, prior to reproduction, which were growing in the soil (2.5 months after seeding), were used in the present work. The 11th and 16th leaf blades and the 7th, 10th and 15th stem internodes, counting from the smallest recognizable leaf (green blade of ~1–2 mm in length) at the top of the plants, were used as materials.

### 4.2.2. Hardness test

The hardness levels of the leaves and stems of plants were measured as force (Newton, N) using a Compact Table-Top Tensile Tester EZ-SX 500N (Shimadzu Co., Kyoto, Japan) controlled by the RAPEZIUM X software for Windows (Shimadzu Co.). To determine the hardness of leaves and stems, penetration and bending tests, respectively, were employed. In the penetration test for leaf, a 3-mm diameter stainless-steel rod was used to make a hole in the 11th and 16th leaves by applying pressure from the adaxial side. The leaves were placed on a 52-mm diameter cylinder with a 5-mm diameter hole in the center and then were penetrated by the stainless-steel rod. In the three-point bending test for stem, the stem segments, which included 10th or 15th internodes, were laid sideways like a bridge on two acrylic boards (each 10 mm thick) vertically standing at intervals of 20 mm. The stems were folded until they were

broken with a wedge (20-mm width, 8-mm depth and 14-mm height; cutting edge part, 20-mm width, 8-mm depth, 8-mm height, and 45° edge angle) at the distal end of the 5-mm diameter stainless-steel rod. To measure the hardness of the resilient seventh internode, the folding test without breaking was carried out. The stems, including seventh internodes, were pushed with the wedge described above until a 1-cm fold occurred. Plant materials derived from at least three independent plants were used for each measurement.

### 4.2.3. Transmission electron microscopy (TEM)

The 11th leaf blades and the 10th and 15th stem internodes of the pBIN19- and the *hUGT1*-transgenic tobacco plants cultured in soil were cut into small pieces. The pieces were immersed overnight in a prefixation solution [0.1 M sodium cacodylate buffer (pH 7.2), 2.5% (v/v) glutaraldehyde] under reduced pressure by vacuum-infiltration and subsequently washed with 0.1 M sodium cacodylate buffer. Samples were postfixed in 1.5% (w/v) $OsO_4$ for 2 h in 0.1 M sodium cacodylate buffer on ice and then dehydrated in a graded ethanol series [50%, 70%, 80%, 90%, 95% and 100% (v/v)]. The samples were substituted with an ethanol–propylene oxide mixture (1:1) once and with propylene oxide twice, and embedded in EPOK 812 resin (Oken Shoji, Tokyo, Japan) at 60°C for 24 h. Ultra-thin sections (70 to 80 nm thick) were obtained with a diamond knife on an Ultracut E ultramicrotome (Reichert-Jung, Vienna, Austria), then stained with 2% uranyl acetate for 10 min and lead citrate for 5 min, and finally examined with a JEM 1200EX or JEM1400 transmission electron microscope (JEOL, Tokyo, Japan) at 80 kV.

The cell wall thicknesses were determined by measuring at 10 different locations along the cell wall in each of the more than 100 electron microscopic images using ImageJ software (https://imagej.nih.gov/ij/). Then, the means and standard deviations were calculated.

### 4.2.4. Extraction of total cell wall materials (TCWMs)

Before the extraction of TCWMs, the fresh weights (FWs) of the 11th and 16th leaves, and the 10th and 15th stem internodes, of soil-cultured plants were measured. Then, after air-drying for 16 h at 65°C in a dry oven, the dry weights (DWs) of these leaves and stem internodes were measured. The percentage DW/FW (%) was calculated as the ratio of DW to FW for each plant material. To extract TCWMs from plant samples, the method devised by Foster et al. (48) was employed with several modifications, as described in our previous report (86). In total, 60 mg of air-dried leaves and stem internodes was used for extraction. The final extracted weight of the TCWMs was calculated on a FW basis. Plant materials derived from at least three independent plants were used for each measurement.

### 4.2.5. Quantification of lignin and RT-PCR analysis of lignin biosynthetic genes

For lignin extractions, 10 mg of air-dried samples harvested from the 11th and 16th leaves, and the 10th and 15th internodes, of the pBIN19- and the *hUGT1*-transgenic tobacco plants cultured in soil were used. These samples were ground with 5-mm stainless balls in a 2-mL screw-cap tube (Watson, Tokyo, Japan) using a bead crusher μT-12 (TAITEC Corp., Saitama, Japan) at 2,600 rpm for 1 min. The quantification of lignin was carried out by modifying the thioglycolic acid method described by Bonawitz et al. (87). Finally, based on the lignin standard (Nacalai Tesque Inc., Kyoto, Japan), the lignin content in each of the samples was calculated on a FW basis.

To determine the transcriptional levels of lignin biosynthetic genes by reverse transcription (RT)-PCR, total RNAs were isolated from the 5th leaves of the pBIN19- and the *hUGT1*-transgenic tobacco plants cultured in soil using a NucleoSpin RNA Kit (Macherey-Nagel GmbH & Co. KG., Duren, Germany) according to the manufacturer's instructions. Aliquots (1 μg) of the total RNA samples were used as templates for cDNA synthesis with ReverTra Ace (TOYOBO Co., Ltd., Osaka, Japan) using an oligo-dT 17-mer primer. Six sets of primers, which were specific for five tobacco enzyme genes

encoding phenylalanine ammonia-lyase (NtPAL), cinnamate 4-hydorxylase (NtC4H), 4-coumarate:CoA ligase (Nt4CL), cinnamoyl-CoA reductase (NtCCR), and cinnamyl alcohol dehydrogenase (NtCAD) in the lignin biosynthetic pathway (87) and the internal control, an elongation factor-1α gene (*EF-1α*) of tobacco, shown in Table 4.1, were used for the quantitative PCR (qPCR) analysis with the cDNA described above. The qPCR analysis was carried out using PowerUp™ SYBR™ Green Master Mix (ThermoFisher Scientific, Waltham, MA, USA) with StepOnePlus™ system (Applied Biosystems, Foster City, CA, USA). The steps and cycles for qPCR were as follows; 50°C for 2 min on hold for the activation of uracil-DNA glycosylase (UDG); 95°C for 2 min on hold for the activation of Dual-Lock™ DNA polymerase; 40 cycles of 95°C for 15 s, 55°C for 15 s and 72°C for 1 min for qPCR; and one cycle of 95°C for 15 s, 60°C for 1 min and 95°C for 15 s (3% ramp rate between 60°C and 95°C) for the melt curve. The qPCR data were analyzed with Comparative Ct (ΔΔCT) using StepOne™ software. The means and the standard deviations were obtained from three independent experiments.

### 4.2.6. Statistical analysis

The statistical analysis was performed using a one-way analysis of variance (ANOVA) employing the *F*-test (88) for comparisons among the plant lines. Tukey's honestly significant difference (HSD) test ($\alpha = 0.05$ as the significance level) was carried out as the post-hoc test. In each experiment, an adequate number of samples obtained from three independent plants in the wild type, pBIN19-transgenic control and three *hUGT1*-transgenic lines were used.

**Table 4.1.** Primers for RT-PCR of lignin biosynthetic genes.

| Target (Accession No. of GenBank) | Primer names | Sequences | Sizes (bps) |
|---|---|---|---|
| D63396.1 | NtEF-1α-RT-F | 5′-TGGACAGACCCGTGAACATG-3′ | 80 |
| | NtEF-1α-RT-R | 5′-CATCCATCTTGTTACAGCAGCAA-3′ | |
| AB008199.1 | NtPAL-RT-F | 5′-TGCTAATGTTCTCGCGGTCTT-3′ | 80 |
| | NtPAL-RT-R | 5′-CAGTGAACTCGGGCTTTCCA-3′ | |
| NM001325516.1 | NtC4H-RT-F | 5′-GACTGAACCAGACACCCACA-3′ | 80 |
| | NtC4H-RT-R | 5′-GAGGAATTGCCATACGGAGA-3′ | |
| U50845.1 | Nt4CL-RT-F | 5′-AATTTGACATTGCTCCGTTCCT-3′ | 80 |
| | Nt4CL-RT-R | 5′-CAGAACAATAGGCGGCACAA-3′ | |
| A86534.1 | NtCCR-RT-F | 5′-TCGCCTCTTGGCTCGTTAAA-3′ | 80 |
| | NtCCR-RT-R | 5′-TTTCCGATCATCTGGATTTCG-3′ | |
| X62344.1 | NtCAD-RT-F | 5′-CAGCTATTGGTTGGGCTGCTA-3′ | 80 |
| | NtCAD-RT-R | 5′-TTCAGGTCCTGTGTTTCTGAGAGT-3′ | |

## 4.3. Results

### 4.3.1. *hUGT1*-transgenic plants show enhanced hardness

I selected three *hUGT1*-transgenic tobacco (*N. tabacum* cv. SR-1) plant lines (Nos. 2, 4 and 23) obtained by leaf disc inoculation with *Agrobacterium tumefaciens* strain LBA4404 harboring pBIN19 or pBIN-hUGT1 (13). T1 plants of each line were transplanted into soil in pots for cultivation. These transgenic plants outwardly displayed no phenotypic differences, except for an enhanced growth rate and darker green leaves, as described previously, compared with wild type plants and pBIN19-transgenic control plants during cultivation in soil for 2 months (13). However, the *hUGT1*-transgenic plants appeared to be robust overall, with thick leaves and stems rigid to the touch, compared with wild type plants and pBIN19-transgenic controls.

To determine the hardness of the leaves and stems of *hUGT1*-transgenic plants, a hardness test using a tensile tester machine controlled by analytical software was performed. I chose the 15th internode, counting from the smallest recognizable leaf (green blade of ~1–2 mm in length) at the top of the plants, because it was the midstem position of vegetatively growing tobacco plants used in my study, and similar to the 10th internode (counting from the first fully opened leaf at the top) position in the early research on alterations of lignin biosynthesis using transgenic tobacco plants by Swalt et al. (89). Because the 15th internode is structurally developed, I chose the 10th internode as a younger, immature position, in which the early stage of secondary xylem differentiation was progressing. For leaves, the 11th leaf (counted in the same way as the internodes) was used as the young leaf material because it almost fully expanded, while the 16th leaf was used as the mature but not aged leaf material. Initially, I investigated the hardness of wild type tobacco plants without any transgenes. In the hardness tests, the 11th and 16th leaves of wild type tobacco plants showed 1.08 N and 1.01 N, respectively, while the 10th and 16th internodes showed 14.53 N and 19.05 N, respectively (Table 4.2). The hardness of young stem (7th internode) was 1.92 N. Next, I carried out the hardness test using pBIN19-transgenic tobacco plants. The 11th and 16th leaves of pBIN19 transgenic control plants showed 1.07 N and 1.18 N, respectively, while the 10th and 16th internodes showed 19.71 N and 21.86 N, respectively (Table

4.2). No significant difference in hardness was found between the leaves of wild type and pBIN19-control plants. The hardness of the young stem (7th internode) of pBIN19-transgenic plants was 2.75 N, but there was no significant difference between the wild-type and pBIN19-transgenic plants. Thus, the hardness of pBIN19-transgenic plants was similar to that of wild type plants, although, as a whole, the pBIN19-transgenic control line chosen in my study seemed to have a slightly rigid trait. However, even with the differences between lines, there was no possibility that the inserted T-DNA, including the kanamycin resistant gene, in the pBIN19-transgenic plants caused a significant alteration in plant hardness. Thus, I decided to use this pBIN19-transgenic plant line as a control instead of wild type plants in subsequent experiments.

The hardness tests revealed that the *hUGT1*-transgenic tobacco plants were more robust than the pBIN19-transgenic control plants, as well as the wild type plants. On 2.5-month-old *hUGT1*-transgenic plants, the 11th leaves of lines 2 and 23 were 1.19- and 1.32-fold, respectively, greater than those of the control plants (Table 4.2). However, the 16th leaf of line 23 was also 1.14-fold greater, although the 16th leaves of all the transgenic lines did not show enhanced hardness compared with the control plants (Table 4.2). Thus, the enhanced hardness of young leaves of *hUGT1*-transgenic plants was caused by an increase in cell wall thickness, cell wall strength or both.

The stem hardness of *hUGT1*-transgenic plants was also enhanced. Because there was no difference in stem diameters between the pBIN19- and the *hUGT1*-transgenic plants (Table 4.3), the enhanced stem hardness appeared to be a trait of *hUGT1*-transgenic plants. The 10th internodes of 2.5-month-old *hUGT1*-transgenic plants were 1.06- to 1.50-fold harder than those of pBIN19-transgenic plants. Similar levels of increased hardness were found in the bending test using the 15th internodes of 2.5-month-old *hUGT1*-transgenic plants, although the hardness levels of internodes of both *hUGT1*-transgenic and control plants were slightly increased (Table 4.2). Even though the xylem areas at their 15th internodes were 1.67- to 1.89-fold wider than at their 10th internodes (Table 4.4), there was no significant difference in the strengths. It may be that, although the xylem area was structurally developed, it had not reached

maturity. Furthermore, the hardness of young stems (seventh internode) of the 2.5-month-old *hUGT1*-transgenic plant lines examined was similarly greater, by 1.08- to 1.77-fold, than those of control plants (Table 4.2). The increased stem hardness of *hUGT1*-transgenic plants may be caused by an increase in cell wall thickness and/or cell wall materials, as seen in the leaf, but the mechanisms in the leaves and stems might be different because the increased stem hardness in the *hUGT1*-transgenic plants was maintained even as they developed.

### 4.3.2. Increased cell wall thickness in leaves and stems of *hUGT1*-transgenic plants

Although other reasons are possible, an increase in cell wall strength or cell wall thickness is the most likely cause of the enhanced hardness. Because the strength of the cell wall could not be directly measured, the possibility of alterations in cell wall thickness in the *hUGT1*-transgenic plants was investigated. To determine the cell wall thickness, TEM was used to directly analyze the cell architecture in leaves and stems of pBIN19- and *hUGT1*-transgenic plants. The cell wall thickness of mesophyll cells in palisade tissues of leaves, and cortical cells close to the outer phloem parenchyma and xylem fiber cells in stems, were measured at more than 10 locations per TEM image.

In the palisade tissue of the leaves, the average cell wall thickness between two adjacent cells was greater in the *hUGT1*-transgenic plants than in the control plants (Table 4.5). However, because the boundaries of the cell walls between each adjacent cell were not clear, the cell wall thickness could not be accurately measured. Furthermore, because the two cells were pushed together, the cell wall thickness differed from place to place. Thus, the cell wall thicknesses of cells facing the intercellular space were measured. The TEM analysis revealed that the cell walls of leaves in the *hUGT1*-transgenic plants were thicker than those of pBIN19-transgenic plants (Fig. 4.1A–D). The cell wall thicknesses of palisade tissue cells in the 11th leaves of *hUGT1*-transgenic plant lines 2 and 23 were 132 nm and 127 nm, respectively, and that of pBIN19-transgenic control leaves was 94 nm (Fig. 4.1A–D, Table 4.6). Thus, the leaves of the former were 1.40- and 1.35-fold thicker, respectively.

**Table 4.2.** Hardness tests on leaves and stems of pBIN19- and *hUGT1*-transgenic plant lines

| Organ | Position | Mean ± standard deviation (*N*) | | | | |
|---|---|---|---|---|---|---|
| | | Wild type | pBIN19 | *hUGT1*-2 | *hUGT1*-4 | *hUGT1*-23 |
| Leaf | 11th | 1.08 ± 0.04c | 1.07 ± 0.10c | 1.27 ± 0.03ab | 1.10 ± 0.05bc | 1.41 ± 0.08a |
| | 16th | 1.01 ± 0.07b | 1.18 ± 0.02ab | 1.19 ± 0.05ab | 1.10 ± 0.08ab | 1.34 ± 0.17a |
| Stem internode | 10th | 14.53 ± 2.21c | 19.71 ± 6.05bc | 29.62 ± 4.36a | 20.85 ± 3.28abc | 25.52 ± 4.49ab |
| | 15th | 19.05 ± 2.48c | 21.86 ± 2.69bc | 31.09 ± 3.69a | 27.68 ± 0.30ab | 27.33 ± 4.26ab |
| | 7th | 1.92 ± 0.31c | 2.75 ± 0.13bc | 2.96 ± 0.71bc | 3.77 ± 0.40ab | 4.87 ± 1.08a |

In each test, the mean and standard deviation of three independent plants in wild type, pBIN19-transgenic control, and each of the *hUGT1*-transgenic plant lines were calculated. For comparison among the plant lines, a one-way ANOVA employing the F-Test (88) was used. Tukey's HSD test was carried out as the post-hot test. Different lower-case letters indicate significant difference ($P$<0.05) among the plant lines.

**Table 4.3.** Stem diameters of pBIN19- and *hUGT1*-transgenic plant lines

| Organ | Position | Mean ± standard deviation (nm) | | | | |
|---|---|---|---|---|---|---|
| | | Wild type | pBIN19 | *hUGT1*-2 | *hUGT1*-4 | *hUGT1*-23 |
| Stem internode | 10th | 5.64 ± 0.43a | 5.99 ± 0.31a | 5.69 ± 0.29a | 6.13 ± 1.04a | 5.84 ± 0.30a |
| | 15th | 5.57 ± 0.25a | 5.60 ± 0.58a | 5.90 ± 0.24a | 6.24 ± 0.34a | 5.82 ± 0.68a |

The means and standard deviations of the diameters of four stem internode slices cut from three independent plants of each line were calculated. For comparison among the plant lines, a one-way ANOVA employing the F-Test (88) was used. Tukey's HSD test was carried out as the post-hot test. Different lower-case letters indicate significant difference ($P$<0.05) among the plant lines.

**Table 4.4.** Widths of xylem areas in stems of pBIN19- and *hUGT1*-transgenic plant lines

| Organ | Position | Mean ± standard deviation (μm) | | | | |
|---|---|---|---|---|---|---|
| | | Wild type | pBIN19 | *hUGT1*-2 | *hUGT1*-4 | *hUGT1*-23 |
| Stem internode | 10th | 186.8 ± 7.6a | 187.9 ± 23.5a | 205.7 ± 25.6a | 199.0 ± 54.9a | 202.4 ± 11.8a |
| | 15th | 332.1 ± 63.5a | 322.7 ± 9.0a | 389.4 ± 37.4a | 332.8 ± 85.0a | 367.1 ± 6.9a |

The means and standard deviations of the diameters of four stem internode slices cut from three independent plants of each line were calculated. For comparison among the plant lines, a one-way ANOVA employing the F-Test (88) was used. Tukey's HSD test was carried out as the post-hot test. Different lower-case letters indicate significant difference ($P$<0.05) among the plant lines.

**Table 4.5.** Cell wall thicknesses of pBIN19- and *hUGT1*-transgenic plant lines

| Organ | Mean ± standard deviation (nm) | | | |
|---|---|---|---|---|
| | pBIN19 | *hUGT1*-2 | *hUGT1*-4 | *hUGT1*-23 |
| Leaf (11th)<br>(palisade tissue, double) nm | 98.8 ± 17.9b | 146.3 ± 49.1a | 100.7 ± 26.7b | 115.7 ± 28.3b |

The means and standard deviations of cell wall thickness were calculated from more than 100 electron microscopic images of each line. For comparison among the plant lines, a one-way ANOVA employing the F-Test (88) was used. Tukey's HSD test was carried out as the post-hot test. Different lower-case letters indicate significant difference ($P$<0.05) among the plant lines.

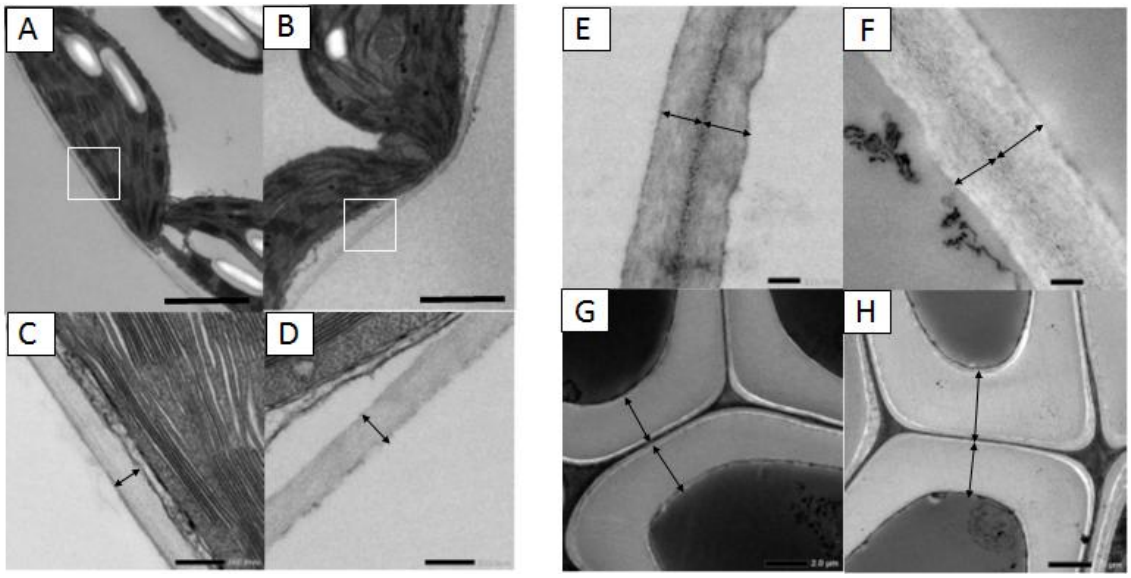


**Fig. 4.1.** Cell walls of the pBIN19-transgenic and the *hUGT1*-transgenic tobacco plants observed by transmission electron microscopy. (A– D) Mesophyll cells facing the intercellular space in palisade tissues of 11th leaves. (A and C) pBIN19-transgenic plant and (B and D) *hUGT1*-transgenic plant line 23. (C and D) High-power magnifications of the boxes shown in (A) and (B), respectively. (E and F) Cortical cells close to the outer phloem parenchyma of 10th internodes in stems of the pBIN19-transgenic (E) and the *hUGT1*-transgenic plant (F). (G and H) Xylem fibers of 10th internodes in stems of the pBIN19-transgenic (G) and the *hUGT1*-transgenic plant (H). Arrows indicate the cell wall width. Scale bars: A and B, 2.0 μm; C– F, 200 nm; G and H, 2.0 μm.

Cortical cells close to the outer phloem were used to observe the primary cell walls of the stems (Fig. 4.1E and F). The cell wall thickness of cortical cells in the 10th internode of the stem was 1.18-fold greater in *hUGT1*-transgenic plant line 4 than in pBIN19-transgenic plants, but there were no significant differences between transgenic lines 2 and 23 and the pBIN19-transgenic plants (Table 4.6). Although the cell wall thicknesses of cortical cells in 15th internodes of both *hUGT1*-transgenic and control plants were similar or slightly decreased, the difference in the cell wall thickness between the *hUGT1*-transgenic plants and the control plants was more pronounced. Additionally, the cell wall thicknesses of xylem fiber cells of *hUGT1*-transgenic plants increased (Fig. 4.1G and H). The increased thicknesses of 10th internodes in the *hUGT1*-transgenic lines 2, 4 and 23 were 1.28-, 1.09- and 1.14-fold, respectively (Table 4.6). For the 15th internode, lines 2 and 23 showed 1.36- and 1.12-fold increases, but line 4 showed a thickness similar to the control (Table 4.6). Thus, the cell wall thicknesses of both leaves and stems increased, which was expected based on the hardness tests described above.

### 4.3.3. Increased cell wall accumulation in *hUGT1*-transgenic plants

Because the TEM analysis revealed that the cell wall thickness of *hUGT1*-transgenic plants was increased, it was hypothesized that the amounts of cell wall materials was also increased. Thus, the total cell wall materials (TCWMs) in the *hUGT1*-transgenic and the control plants were extracted for quantification. The results of two quantifications are shown in Table 4.7. The 11th and 16th leaves, and 10th and 15th stem internodes, from each plant were dried to determine their DWs. The DW/FW values of the 11th and 16th leaves in the *hUGT1*-transgenic lines were 1.17- to 1.25-fold and 1.10- to 1.28-fold greater than those of the pBIN19-transgenic plants, respectively. Thus, the solid content in the leaves of *hUGT1*-transgenic plants was always greater than that of the leaves of control plants. However, the DW/FW values of the 16th leaves were lower than those of the 11th leaves in both plants, indicating that the former contained a greater moisture content.

**Table 4.6.** Cell wall thicknesses of pBIN19- and *hUGT1*-transgenic plant lines

| Organ (Tissue) | Position (unit) | Mean ± standard deviation | | | |
|---|---|---|---|---|---|
| | | pBIN19 | *hUGT1-2* | *hUGT1*-4 | *hUGT1*-23 |
| Leaf (palisade tissue) | 11th (nm) | 93.9 ± 13.0c | 131.9 ± 15.6ab | 93.7 ± 10.6bc | 127.2 ± 12.8a |
| Stem (cortex) | 10th (nm) | 307.5 ± 64.5b | 332.4 ± 40.7ab | 364.3 ± 110.8a | 323.8 ± 88.4ab |
| | 15th (nm) | 251.6 ± 35.8b | 333.7 ± 24.0a | 305.3 ± 60.9a | 358.4 ± 68.6a |
| Stem (xylem fiber) | 10th (μm) | 2.050 ± 0.282b | 2.622 ± 0.392a | 2.551 ± 0.368a | 2.330 ± 0.288a |
| | 15th (μm) | 2.182 ± 0.326b | 2.974 ± 0.607a | 2.168 ± 0.208ab | 2.449 ± 0.238ab |

The means and standard deviations of the cell wall thickness were calculated from more than 100 electron microscopic images of each line. For comparison among the plant lines, a one-way ANOVA employing the F-Test (88) was used. Tukey's HSD test was carried out as the post-hot test. Different lower-case letters indicate significant difference ($P$<0.05) among the plant lines.

The amounts of the FWs that were constituted by TCWMs in the 11th leaves of the *hUGT1*-transgenic lines were 1.21- to 1.38-fold greater than those of the pBIN19-transgenic plants. This increase in the TCWMs of the leaves of *hUGT1*-transgenic plants may result from the increased cell wall thickness observed in the TEM. However, even though the amounts of the FWs that were constituted by TCWMs in the 16th leaves in the *hUGT1*-transgenic lines were 1.09- to 1.33-fold greater than those of pBIN19-transgenic plants, the TCWM amounts themselves were less than those of the 11th leaves. The decreases in these amounts appeared to be related to the expansion of the vacuoles and the increase in the moisture content during the maturation of the 16th leaves. This was corroborated by the decrease in the amount of TCWMs in the DW/FW value. The increase in the moisture contents of the 16th leaves reduced the hardness compared with younger leaves but caused no difference in leaf hardness between the *hUGT1*-transgenic and control plants, as mentioned previously (Table 4.2).

The DW/FW values of the 10th and 15th internodes of stems in the *hUGT1*-transgenic lines were 0.92- to 1.26-fold and 0.97- to 1.27-fold greater compared with those of pBIN19-transgenic plants, respectively (Table 4.7). Thus, in the case of stems, because the moisture content in each sample fluctuated considerably, the solid contents of *hUGT1*-transgenic plants did not appear to be greater than those of control plants, unlike for the leaves. The 10th internodes of *hUGT1*-trangenic plants generally showed increased amounts of TCWMs compared with those of control plants. This result supported the enhanced hardness of the 10th internodes of *hUGT1*-transgenic plants. In both the *hUGT1*-transgenic and control plants, the amounts of TCWMs in the 15th internodes were 1.56- to 1.99-fold greater than those of the 10th internodes (Table 4.7). For stems, although there was an increase in the thickness of the primary cell wall, the secondary cell wall appeared to constitute most of the cell wall. Thus, the increase in the cell wall amount showed here resulted from the increase in the amount of secondary cell wall. However, because there was almost no difference in the thickness of the secondary cell wall between the 10th and the 15th internodes, it was hypothesized that the increase in the amounts of TCWMs in the 15th internodes resulted from an increased number of xylem cells. Indeed, the widths of the xylem areas in the 15th

internodes were greater than those in the 10th internodes (Table 4.4). However, the amounts of TCWMs in the 15th internodes were similar between the *hUGT1*-transgenic and the control plants (Table 4.7). This result conflicted with the difference in hardness found in the 15th internodes between the *hUGT1*-transgenic and the control plants.

Although there are still points to be resolved, these results demonstrated that the increased amount of cell wall materials resulted from the increased cell wall thickness in *hUGT1*-transformed plants. This appears to be one reason for the enhanced hardness of *hUGT1*-transgenic plants.

In previous report, an increased accumulation of lignin was observed in the leaves of *hUGT1*-transgenic plants (13). Thus, the enhanced hardness of the leaves and stems of *hUGT1*-transgenic plants may be explained by the increased accumulation of lignin. To confirm the increased accumulation of lignin, lignin was extracted from the 11th and 16th leaves, and the 10th and 15th stem internodes. The lignin contents in the 11th and 16th leaves of *hUGT1*-transgenic plants were significantly greater than those of the control plants (Table 4.8), as reported previously (13). The contents in the 11th and 16th leaves of *hUGT1*-transgenic plants were 1.27- to 1.37-fold and 1.27- to 1.34-fold greater, respectively, compared with those of the control. Thus, the increased lignin content may be a reason for the enhanced hardness of the leaves of *hUGT1*-transgenic plants. However, the lignin contents of the 16th leaves of the *hUGT1*-transgenic plants decreased compared with in the 11th leaves, resulting in a reduction in the hardness of the 16th leaves. The decrease in the lignin content may be related to an increase in the cells' moisture contents, which was already shown by the decrease in cell wall mass, and finally, the difference in hardness between the *hUGT1*-transgenic and the control plants was reduced or disappeared.

### 4.3.4. Enhanced lignification in leaves and stems of *hUGT1*-transgenic plants

For stems, the lignin contents of the *hUGT1*-transgenic plants were also greater than those of control plants.

**Table 4.7.** Amounts of total cell wall materials (TCWMs) in growing pBIN19- and *hUGT1*-transgenic plant lines

| Organ | | | | Mean ± standard deviation | | | |
|---|---|---|---|---|---|---|---|
| | | | | pBIN19 | *hUGT1*-2 | *hUGT1*-4 | *hUGT1*-23 |
| Leaf | 11th | DW/FW (%) | 1st | 6.5 ± 0.6b | 8.1 ± 0.3a | 7.6 ± 0.3a | 7.9 ± 0.5a |
| | | | 2nd | 5.7 ± 1.3a | 6.8 ± 0.4a | 7.0 ± 0.4a | 6.9 ± 0.8a |
| | | TCWM in FW (mg/g) | 1st | 32.6 ± 3.8b | 41.9 ± 5.1a | 39.3 ± 2.3ab | 39.4 ± 5.5ab |
| | | | 2nd | 30.3 ± 10.4b | 37.2 ± 1.6ab | 41.9 ± 3.7a | 41.9 ± 3.6a |
| | 16th | DW/FW (%) | 1st | 4.6 ± 0.4b | 5.9 ± 0.2a | 5.7 ± 0.2a | 5.7 ± 0.3a |
| | | | 2nd | 5.1 ± 1.0b | 5.6 ± 0.4ab | 5.9 ± 0.6ab | 6.5 ± 0.7a |
| | | TCWM in FW (mg/g) | 1st | 21.7 ± 2.6b | 27.7 ± 3.0a | 28.6 ± 3.6a | 28.0 ± 2.4a |
| | | | 2nd | 19.2 ± 2.7b | 20.9 ± 2.0ab | 23.5 ± 2.7ab | 25.6 ± 3.5a |
| Stem internode | 10th | DW/FW (%) | 1st | 4.7 ± 0.2a | 5.9 ± 0.4a | 5.4 ± 0.6a | 5.2 ± 0.8a |
| | | | 2nd | 6.2 ± 0.6a | 6.7 ± 0.1ab | 5.7 ± 0.6a | 5.8 ± 0.6ab |
| | | TCWM in FW (mg/g) | 1st | 19.2 ± 1.0a | 28.5 ± 3.3a | 24.5 ± 8.4a | 22.5 ± 4.3a |
| | | | 2nd | 27.7 ± 3.6a | 30.7 ± 2.1a | 22.8 ± 4.6a | 26.7 ± 6.7a |
| | 15th | DW/FW (%) | 1st | 5.9 ± 0.2b | 7.5 ± 0.5a | 6.2 ± 1.0ab | 6.5 ± 0.2ab |
| | | | 2nd | 7.8 ± 1.2a | 8.6 ± 0.7a | 7.6 ± 0.4a | 7.6 ± 0.6a |
| | | TCWM in FW (mg/g) | 1st | 38.2 ± 1.7a | 48.5 ± 0.4a | 41.5 ± 10.5a | 39.5 ± 6.6a |
| | | | 2nd | 44.9 ± 7.5a | 48.0 ± 1.9a | 41.6 ± 1.5a | 43.3 ± 1.2a |

The means and standard deviations of at least three repeated determinations from two independent samples were calculated. For comparison among the plant lines, a one-way ANOVA employing the F-Test (88) was used. Tukey's HSD test was carried out as the post-hot test. Different lower-case letters indicate significant difference ($P$<0.05) among the plant lines.

Although the statistical significance of the difference in the 10th internode was unclear, the 10th and 15th internodes of the *hUGT1*-transgenic lines showed greater lignin contents compared with those of the control. These greater lignin contents in the 10th and 15th internodes of the *hUGT1*-transgenic plants might influence the hardness. The lignin contents in the 15th internodes of both the *hUGT1*-transgenic and the control plants were 2.11- to 3.44-fold more than in the 10th internodes. However, the greater lignin contents in the 15th internodes did not correlate with a significant increase in the hardness. The hardness of the 15th internodes was only slightly increased compared with that of the 10th internodes. Based on the above results, it was hypothesized that the enhanced accumulation of lignin was promoted by *hUGT1* expression in tobacco plants and that this accumulation was one reason for the increased hardness of *hUGT1*-transgenic plants.

### 4.3.5. Up-regulation of lignin biosynthetic genes in *hUGT1* transgenic plants

*hUGT1* expression in plant cells promoted an increase in lignin accumulation. Thus, I investigated whether the transcription of genes in the lignin biosynthetic pathway was activated in *hUGT1*-transgenic plants (Fig. 4.2A). A qRT-PCR analysis was performed using total RNA from the *hUGT1*-transgenic plants, as well as the control plants, and specific primer sets for the key tobacco lignin biosynthesis enzyme genes encoding NtPAL, NtC4H, Nt4CL, NtCCR and NtCAD. The qRT-PCR analysis revealed that four of the five lignin biosynthetic genes were up-regulated in the three *hUGT1*-transgenic lines (Fig. 4.2B). The levels of *NtPAL*, *NtC4H*, *Nt4CL* and *NtCCR* were up-regulated 1.2- to 1.9-fold, 1.3- to 1.8-fold, 1.4- to 1.7-fold and 1.6- to 2.0-fold, respectively, compared with the control, whereas that of *NtCAD* was similar to the control (Fig. 4.2B). The up-regulated level of each enzyme gene was not high but may be sufficient to increase the lignin content in leaves, which hardly accumulate lignin. Thus, the *hUGT1* expression in tobacco cells may stimulate the lignin biosynthetic pathway at the transcriptional level.

**Table 4.8.** Lignin contents in leaves and stems of pBIN19- and *hUGT1*-transgenic plant lines

| Organ | Position | Mean ± standard deviation (μg/mg FW) | | | |
|---|---|---|---|---|---|
| | | pBIN19 | *hUGT1*-2 | *hUGT1*-4 | *hUGT1*-23 |
| Leaf | 11th | 2.33 ± 0.49b | 2.96 ± 0.16ab | 3.19 ± 0.57a | 3.17 ± 0.20a |
| | 16th | 1.81 ± 0.34b | 2.35 ± 0.09a | 2.30 ± 0.11a | 2.42 ± 0.29a |
| Stem internode | 10th | 2.06 ± 0.34a | 2.97 ± 0.39a | 3.24 ± 1.44a | 2.52 ± 0.82a |
| | 15th | 6.73 ± 0.46b | 9.17 ± 0.96a | 6.84 ± 0.88b | 8.66 ± 0.83a |

The means and standard deviations of at least three repeated determinations were calculated. For comparison among the plant lines, a one-way ANOVA employing the F-Test (88) was used. Tukey's HSD test was carried out as the post-hot test. Different lower-case letters indicate significant difference ($P$<0.05) among the plant lines

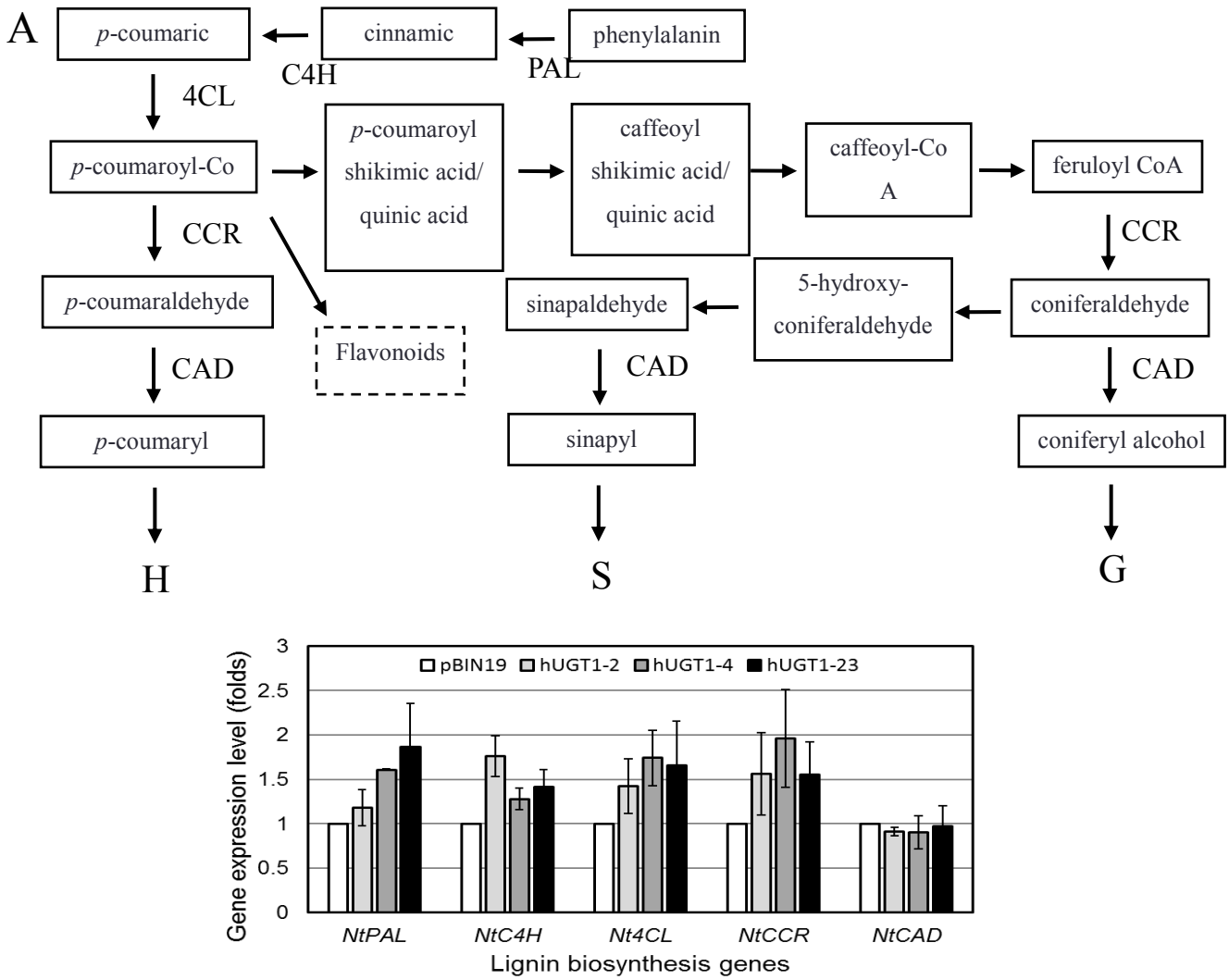


**Fig. 4.2.** Enhanced lignification of *hUGT1*-transgeic plants. (A) Lignin biosynthetic pathway (87). PAL, phenylalanine ammonia-lyase; C4H, cinnamate 4-hydorxylase; 4CL, 4-coumarate:CoA ligase; CCR, cinnamoyl-CoA reductase; CAD, cinnamyl alcohol dehydrogenase; H lignin, *p*-hydroxyphenyl lignin; S lignin, syringyl lignin; G lignin, guaiacyl lignin. (B) qRT-PCR analysis using *Nicotiana tabacum* primers specific for *NtPAL*, *NtC4H*, *Nt4CL*, *NtCCR* and *NtCAD19* genes, which encode tobacco homologs of the lignin biosynthetic enzymes shown in (A). The tobacco elongation factor-1α (EF-1α) was used as an internal control. A pBIN19-transgenic control and three *hUGT1*-transgenic plants (lines 2, 4 and 23) were used. The nucleotide sequences of specific PCR primers for each gene and their amplicon sizes are listed in Table 4.1. The data were analyzed with Comparative Ct (ΔΔCT) using StepOne™ software. The means and the standard deviations were obtained from three independent experiments. The error bars represent standard deviations.

## 4.4. Discussion

The *hUGT1*-transgenic plants were harder and more rigid to the touch compared with the pBIN19-transgenic control plants. Here, I demonstrated that the *hUGT1*-transgenic plants showed enhanced hardness in leaves and stems (Table 4.2). Although the hyper-galactosylation of xyloglucan was presumed to cause the enhanced hardness of *hUGT1*-transgenic tobacco (22), the main reasons for their enhanced hardness appears to be the increased thickness of their cell walls (Table 4.6) and the increased accumulation of lignin (Table 4.8). Interestingly, the *hUGT1*-transgenic tobacco plants accumulated more cell wall materials compared with control plants (Table 4.7). The increased cell wall thickness is likely an important reason why the *hUGT1*-transgenic tobacco plants displayed a robust phenotype, including stiffness to the touch and an increased hardness of leaves and stems, although the increased lignin accumulation might also be involved. The amounts of TCWMs in the leaves of *hUGT1*-transgenic plants was up to 1.38-fold greater than in leaves of control plants, suggesting that the *hUGT1*-transgenic plants are a possible resource for increased biomass production.

The overexpression of *hUGT1* caused several significant alterations in transformed tobacco plants. Although the reasons for such unforeseen alterations remain to be determined in future studies, it seems likely that the increased amount of galactose in the hemicellulosic and pectic polysaccharides of the cell wall was not the direct cause of the increased accumulation of cell wall materials. However, since the higher level of galactosylated xyloglucan mechanically enhances the plant body strength (22), this might be a reason for the increased hardness of *hUGT1*-transgenic tobacco. Additionally, a high level of galactosylation of galactose-containing cell wall matrix polymers is related to significant alterations in some signal-transduction pathways, as discussed in my previous report (86). This might be a second reason for the increased hardness.

The hyper-galactosylation of arabinogalactan proteins (AGP) is a third and most probable reason for the increased hardness of *hUGT1*-transgenic tobacco plant. Arabinogalactan is composed of arabinose and galactose and is a type of pectic polysaccharide. Type I arabinogalactan is a side chain on rhamnogalacturonan-I,

whereas type II arabinogalactan is present in AGPs (45). The increased degree of AGP galactosylation might be important because AGPs are candidate mediators of cell–cell interactions and regulators of cell growth (45). In our previous reports, we have shown that AGP polysaccharides are hyper-galactosylated by the expression of *hUGT1* (13,86). It is likely that hyper-galactosylation of AGPs increased in the sensitivity to external signals or hyper-galactosylated AGP molecules themselves acts as functionally enhanced signal molecules to increase in the cell wall thickness and lignin accumulation.

There are some candidate AGPs that may be involved in the increases in primary and secondary cell walls found in the *hUGT1*-transgenic tobacco plants. Some reports suggested that fasciclin-like arabinogalactan (FLA) proteins contribute to not only primary cell wall biosynthesis but also to the biomechanical properties of stems through their impact on the synthesis and architecture of the secondary cell wall (90). For secondary cell wall, stem cell walls of the *Arabidopsis* T-DNA insertion mutants At*fla11* and At*fla12*, and their homozygous At*fla11*/At*fla12* double mutant, showed significant reductions in the concentrations of glucose moieties, which inferred that cellulose deposition was reduced. Furthermore, a tensile strength test revealed that the stems of At*fla11*/At*fla12* double mutants were significantly weaker than those of the wild type (90). These are opposite traits to those found in the *hUGT1*-transgenic tobacco plants. Although the up-regulation of tobacco *FLA11* and *FLA12* orthologs has not been ruled out, their hyper-galactosylation might be involved in the increased cell wall accumulation in *hUGT1*-transgenic plants. In addition, the accumulation of lignin in leaves of the *hUGT1*-transgenic plants was significantly increased. The lignin contents in the leaves and stems of the *hUGT1*-transgenic plants were more than 1.37-fold greater than those of control plants (Table 4.8). The increased lignin content invokes an ectopic accumulation of secondary cell walls in the leaves.

However, because lignin deposits on the primary cell wall are caused by various biotic and abiotic stresses, such as UV irradiation and pathogen infection (87), they might not be related to secondary cell wall accumulation. The TEM analysis indicated that the cell walls of leaf palisade cells in the *hUGT1*-transgenic plants were thicker but

structurally similar to those of the control plants. Furthermore, in my previous report (86), I demonstrated that, except for the increase in the ratio of galactose, the monosaccharide composition in the leaves of *hUGT1*-trangenic plants was the same as that in the leaves of pBIN19-transgenic control plants. Thus, an increased quantity of primary cell wall materials accumulated in the cell walls of *hUGT1*-transgenic plants, resulting in thicker cell walls. *SALT OVERLAY SENSITIVE 5* (*SOS5*, also called *FLA4*) encodes a fasciclin-like AGP, which acts on the same pathway as the leucine-rich repeat receptor kinases FEI1/FEI2 to regulate the biosynthesis of cellulose (perhaps primary cell wall) in *Arabidopsis* (91,92). The hyper-galactoyslation of tobacco SOS5/FLA4 ortholog might be involved in the thicker primary cell wall of *hUGT1*-transgenic plants.

Because the lignin biosynthesis pathway is usually activated in the stem during maturation and there was a possibility that the up-regulation of lignin biosynthesis genes might not be clearly recognized, I decided to use leaves, which hardly accumulate lignin, to investigate gene expression. Furthermore, the lignification of the 11th leaves of the *hUGT1*-transgenic plants was enhanced and the lignin contents of the 16th leaves decreased compared with those of the 11th leaves (Table 4.8), which suggested that the enhanced expression of lignin biosynthetic genes has already occurred younger leaves. Therefore, I chose the 5th leaves as the material for total RNA extractions. In the leaves of *hUGT1*- transgenic plants, the enzyme genes involved in lignin biosynthetic pathway were up-regulated (Fig. 4.2B). Lignin biosynthesis is roughly composed of two pathways; the general phenylpropanoid pathway from phenylalanine to *p*-coumaroyl-CoA and the pathway for monolignol synthesis from *p*-coumaroyl-CoA to three monolignols, p-coumaroyl alcohol, sinapyl alcohol and coniferyl alcohol (20, Fig. 4.2A). Phenylalanine ammonia-lyase (PAL), cinnamate 4-hydorxylase (C4H) and 4-coumarate:CoA ligase (4CL) are involved in the former pathway, while cinnamoyl-CoA reductase (CCR) and cinnamyl alcohol dehydrogenase (CAD) are common enzymes involved in the synthesis of the three monolignols in the latter pathway. PAL may play an important role initiating the first step, while C4H is the rate-limiting enzyme in the lignin biosynthesis pathway (93). The up-regulation of *NtC4H* suggested that the lignin biosynthesis pathway was activated in the leaves of *hUGT1*-transgenic plants. Furthermore, CCR is the enzyme required for the first

lignin-specific step in the phenylpropanoid pathway and has an assumed regulatory function (93). However, *NtCAD* was not up-regulated. CAD seemed to be neither a regulatory nor a key enzyme in terms of carbon allocation to the pathway, and its action is determined by an upstream metabolite process (93). Furthermore, because the decrease in CAD activity to ~7% of wild type seemed to have little effect on the total amount of lignin (93), it is likely that *NtCAD* was expressed sufficiently for the reaction to proceed.

Because the promoters of lignin biosynthesis genes, such as *PAL* and *4CL*, contain several important *cis*-elements to bind MYB transcription factors (MYBs) (94), there is a possibility that the activation of MYBs is responsible for lignin biosynthesis in *hUGT1*-transgenic plants. Because, in *Arabidopsis*, the lignin-specific MYBs, AtMYB58, AtMYB63 and AtMYB85, regulate lignin biosynthesis (94), I will have to confirm whether their tobacco orthologs are up-regulated in my future work.

Khalil et al., have reported that the introduction and expression of heterologous gene *hUGT1* alone causes morphological and physiological changes to tobacco plants (13). Such results suggest the possibility of additional changes in the plants if the loading of UDP-galactose into the Golgi apparatus is more efficient. Because hUGT1 was the first isolated UDP-galactose transporter, this molecule is a typical model for UDP-galactose transporters. Initially, the amino acids essential for the UDP-galactose transport activity of hUGT1 were identified (95). In addition, a detailed analysis of chimeric molecules between hUGT1 and the human CMP-sialic acid transporter revealed which of the 10 transmembrane domains of hUGT1 were essential for the UDP-galactose transporter activity (85) and substrate specificity (39). Furthermore, a heterologous combination between hUGT1 and UDP-galactose:ceramide galactosyltransferase showed that the cellular location of hUGT1 was associated with that of galactosyltransferase, suggesting the pliancy of the hUGT1 function (96). I am aiming to develop a new plant modification method through the hyper-galactosylation of plant cell surfaces, in particular AGPs. For this purpose, the function of the UDP-galactose transporter must be improved. Among the plant UDP-galactose transporters reported, there is no isoform that has been analyzed as well as hUGT1. Additionally, because hUGT1 has been well

characterized, it is considered to be the best material for my purpose. Based on the structure–function relationship of hUGT1, I will be able to obtain hUGT1 with modifications, such as amino acid substitutions and domain exchanges. As the first step, I have already made a modified *hUGT1* having optimal codon usage for plants (artificial *UGT*), and the analysis of its function is in progress.

# Chapter 5. Conclusion

The rising world population leads to increasing food and fuel demands. Dealing with this demand needs increasing plant production. This important challenge has encouraged the scientists to modify cell walls into desired features for more efficient production and utilization. For instance, modifications of the lignin biosynthesis, cellulose deposition, non-cellulosic polysaccharides and cell wall compositions have received significant attention from many researchers all around the world. As these achievements are promising, the modified products would be used not only for cell wall manufacturing but also for the production of super crops.

In my thesis, I accomplished to examine the impact of overexpression of UDP-Gal transporter gene in galactose content of cell wall components. Then I tried to investigate the consequence effect of this cell wall hyper-galactosylation on plant characteristics. The obtained results of my research were described as below.

In chapter 3, I demonstrated that *hUGT1* expression altered the monosaccharide composition of pectin and hemicellulose in the cell wall. Since hUGT1 is responsible for transportation of UDP-Gal from cytosol to Golgi lumen, expression of *hUGT1* resulted in the elevated ratio of galactose to total monosaccharides in the hemicellulose II and pectin fractions of *hUGT1*-transgenic plants compared with that of control plants. Moreover, oligosaccharide mass profiling (OLIMP) revealed a hyper-galactosylation in xyloglucan of hemicellulose II. This change in side chains of xyloglucan could impact the strength of cell wall which might lead to increased hardness in tobacco plants. This possibility was tested in the next step of my study. Finally, I found the enhanced galactose tolerance in *hUGT1*-transgenic plants because of increased galactose incorporation in cell wall via the enhanced UDP-galactose transport from the cytosol to the Golgi apparatus by hUGT1.

In chapter 4, I showed *hUGT1* expression in tobacco plant which led to hyper-galactosylation of non-cellulosic parts of cell wall components, influencing plant hardness. As determined by breaking and bending tests, the leaves and stems of *hUGT1*-transgenic plants were harder than those of control plants. This interesting plant

hardness would be attributed to the positive impact of hyper-galactosylation of side chains of xyloglucan on the strength of cell wall. Furthermore, the transmission electron microscopic analysis showed the increased cell wall thickness in leaves palisade cells and those of cortex cells and xylem fibers in the stem. This result was supported by higher biomass and total cell wall materials extracted from the leaves and stems of *hUGT1*-transgenic plants compared to control plants. Besides, lignin content in cell walls of the *hUGT1*-transgenic elevated which is related to the up-regulation of some genes encoding enzymes in lignin biosynthesis.

Altogether, through this study, the expression of *hUGT1* in tobacco plant verified the key role of the UDP-Gal transporter in galactosylation of cell wall components. As shown in these results, the hyper-galactosylation in pectin and xyloglucan, which are the main Gal acceptors in the cell wall, might result in increasing plant biomass which is caused by the increased cell wall thickness, and consequently enhanced plant hardness. Thus, the remarkable impact of hyper-galactosylation of pectin and xyloglucan on plant growth and development might attribute to an alteration of their probable signaling activity in the plant, which would be an interesting subject of study in future. Furthermore, higher lignification in *hUGT1*-transgenic plants was a notable result of this study. In the future research, the possible relationship between the expression of UDP-Gal transporter genes and the regulation of the genes of lignin biosynthesis should be investigated. In summary, these results may suggest a new novel plant modification strategy that is practical for crop improvement as feedstocks for biofuel production in the future.

## Acknowledgments

Firstly, I would like to express my deep and sincere gratitude to my supervisor Prof. Tanaka for the continuous support of my master and Ph.D. study and related research, for his patience, motivation, and immense knowledge. His friendly guidance and expert advice have been invaluable throughout all stages of the work. It was a great privilege and honor to work and study under his guidance. I have been extremely lucky to have a supervisor who cared so much about my work, and who responded to my questions and queries so promptly. His guidance helped me in all the time of research and writing of this thesis. I am extremely grateful for all he has offered me. I would also like to thank him for his friendship, empathy, and a great sense of humor.

Besides my advisor, I would like to thank the rest of my thesis committee: Prof. Aki and Prof. Kawamoto for reviewing this work and insightful comments and suggestions.

My Special thanks go to assistant professor Kenji Kitamura for his guidance and encouragement who kindly support me through my study. My sincere thanks also go to friendly technician members of genome biotechnology laboratory, Mrs. Hikosaka, Mrs. Koike, Mrs. Ishihara and Mr. Yamaguchi for their guidance and kindness through my work. Without they precious support it would not be possible to conduct this research.

I also thank all the staff of student support center of advanced science of matter faculty for their help and kindness.

I would like to thank my family: my parents for their love, prayers, caring and sacrifices for educating and preparing me for my future. I am very much thankful to my brothers and sisters for supporting me spiritually throughout writing this thesis and my life in general.

Finally, I would like to thank the Japanese government for the scholarship supports of foreign students (MEXT) for providing the funding of my study and life in Japan, which gave me this opportunity to have precious experiences in one of the most world pioneer countries in science and technology.

## References


1. **Hamann, T.**: The plant cell wall integrity maintenance mechanism—concepts for organization and mode of action. Plant Cell Physiol., **56**, 215–223 (2015).

2. **Rose, J. K. C., and Lee, S. J.**: Straying off the highway: trafficking of secreted plant proteins and complexity in the plant cell wall proteome. Plant Physiol., **153**: 433–436 (2010).

3. **Keegstra, K.**: Plant Cell Walls. Plant Physiol.**, 154**: 483–486 (2010).

4. **Somerville, C., Bauer, S., Brininstool, G., Facette, M., Hamann, T., Milne, J., Osborne, E., Paredez, A., Persson, S., Raab, T., Vorwerk, S., and Youngs, H.**: Toward a systems approach to understanding plant cell walls. Science, **306**, 2206–2211 (2004).

5. **Scheller, H.V., and Ulvskov, P.**: Hemicelluloses. Annu.Rev.Plant Biol., **61**, 263–289 (2010).

6. **Höfte, H., and Voxeur, A.**: Plant cell walls. Curr. Biol., **27**, 865–870 (2017).

7. **Wolf, S., Hématy, K. and Höfte, H.**: Growth control and cell wall signaling in plants. Annu. Rev. Plant Biol., **63**, 381–407(2012).

8. **Harholt, J., Suttangkakul, A., and Scheller, H.V.**: Biosynthesis of pectins. Plant Physiol., **153**, 384–395 (2010).

9. **Driouich, A., Follet-Gueye, M.L., Bernard, S., Kousar, S., Chevalier, L., Vicré-Gibouin, M., and Lerouxel, O.**: Golgi-mediated synthesis and secretion of matrix polysaccharides of the primary cell wall of higher plants. Front. Plant Sci., **3**: 79 (2012).

10. **Kleczkowski, L.A., Decker, D., and Wilczynska, M.**: UDP-Sugar pyrophosphorylase: a new old mechanism for sugar activation. Plant Physiol., **156**, 3-10 (2011).

11. **Handford, M., Rodriguez-Furlán, C., and Orellana, A**.: Nucleotide-sugar transporters: structure, function and roles in vivo. Braz. J. Med. Biol. Res., **39**, 1149-1158 (2006).

12. **Reyes, F., and Orellana, A.**: Golgi transporters: opening the gate to cell wall polysaccharide biosynthesis. Current Opin. Plant Biol., **11**, 244–251 (2008).

13. **Khalil, M.F.M., Kajiura, H., Fujiyama, K., Koike, K., Ishida, N., and Tanaka, N.**: The impact of the overexpression of human UDP-galactose transporter gene hUGT1 in tobacco plants. J. Biosci. Bioeng.*,* **109**, 159-169 (2010).

14. **Seifert, G.J.**: Nucleotide sugar interconversions and cell wall biosynthesis: how to bring the inside to the outside. Current Opin. Plant Biol., **7,** 277–284 (2004).

15. **Cosgrove, D.J.**: Growth of the plant cell wall. Nat. Rev. Mol. Cell Biol., **6**, 850–861 (2005).

16. **Pauly, M., and Keegstra, K.**: Plant cell wall polymers as precursors for biofuels. Current Opin. Plant Biol., **13**, 305–312 (2010).

17. **Kaul S., Koo H.L., Jenkins J., Rizzo M., Rooney T., Tallon L.J., Feldblyum T., et al.**: Arabidopsis Genome Initiative. Analysis of the genome sequence of the flowering plant Arabidopsis thaliana. Nature, **408**, 796–815 (2000).

18. **Ouyang S., Liu J., Jones k.m., et al.**: International Rice Genome Sequencing Project. The map based sequence of the rice genome. Nature, **436**, 793–800 (2005).

19. **Tuskan, G.A., Difazio, S., Jansson, S., Bohlmann, j., Grigoriev, I., Hellsten, U., Putnam, N., Ralph, S., Rombauts, S., Salamov, A., et al.**: The genome of black cottonwood, Populus trichocarpa (Torr. & Gray). Science, **313**, 1596–1604 (2006).

20. **Carpita, N., Tierney, M., and Campbell, M.**: Molecular biology of the plant cell wall: searching for the genes that define structure, architecture and dynamics. Plant Mol Biol., **47**, 1–5 (2001).

21. **Strasser, R.**: Plant protein glycosylation. Glycobiology.**, 26**, 926–939 (2016).

22. **Peña, M. J., Ryden, P., Madson, M., Smith, A. C., and Carpita, N. C.**: The galactose residues of xyloglucan are essential to maintain mechanical strength of the primary cell walls in Arabidopsis during growth, Plant Physiol., 134, 443-451 (2004).

23. **Kim, S. K., Kim, D.H., Kim, B.G., Jeon, Y.M., Hong, B.S., and Ahn, J.H**.: Cloning and Characterization of the UDP Glucose/Galactose Epimerases of Oryza sativa. J. Korean Soc. Appl. Biol. Chem., **52**, 315-320 (2009).

24. **Dormann, P., and Benning C.**: The role of UDP- glucose epimerase in carbohydrate metabolism of *Arabidopsis.* Plant J., **13**, 641- 652 (1998).

25. **Orellana, A., Moraga, C., Araya, M., and Moreno, A**.: Overview of nucleotide sugar transporter gene family functions across multiple species. J. Mol. Biol.*,* **428**, 3150–3165 (2016).

26. **Carpita, N. C. and Gibeaut, D. M.**: Structural models of primary cell walls in flowering plants: consistency of molecular structure with the physical properties of the walls during growth. Plant J., **3**, 1-30 (1993).

27. **Reiter, W.-D.**: Biosynthesis and properties of the plant cell wall. Curr. Opin. Plant Biol., **5**, 536-542 (2002).

28. **Keegstra, K. and Raikhel, N.**: Plant glycosyltransferases. Curr. Opin. Plant Biol., **4**, 219-224 (2001).

29. **Berninsone, P. M. and Hirschberg, C. B.**: Nucleotide sugar transporters of the Golgi apparatus. Curr. Opin. Struct. Biol., **10**, 542-547 (2000).

30. **Liu, L., Xu. Y.-X., and Hirschberg, C. B.**: The role of nucleotide sugar transporters in development of eukaryotes. Semin. Cell Dev. Biol., **21,** 600-608 (2010).

31. **Seino, J., Ishii, K., Nakano, T., Ishida, N., Tsujimoto, M., Hashimoto, Y., and Takashima, S.**: Characterization of rice nucleotide sugar transporters capable of transporting UDP-galactose and UDP-glucose. J. Biochem., **148**, 35-46 (2010).

32. **Reyes, F., Marchant, L. Norambuena, L., Nilo, R., Silva, H., and Orellana, A.**: AtUtr1, a UDP-glucose/UDP-galactose transporter from *Arabidopsis thaliana*, is located in the endoplasmic reticulum and up-regulated by the unfolded protein response. J. Biol. Chem., **281**, 9145-9151 (2006).

33. **Norambuena, L., Nilo, R., Handford, M., Reyes, F., Marchant, L., Meisel, L., and Orellana, A.**: AtUTr2 is an *Arabidopsis thaliana* nucleotide sugar transporter located in the Golgi apparatus capable of transporting UDP-galactose. Planta, **222**, 521-529 (2005).

34. **Bakker, H., Routier, F., Oelmann, S., Jordi, W., Lommen, A., Gerardy-Schahn, R., and Bosch, D.**: Molecular cloning of two Arabidopsis UDP-galactose transporters by complementation of a deficient Chinese hamster ovary cell line. Glycobiology, **15**, 193-201 (2005).

35. **Rollwitz, I., Santaella, M., Hille, D., Flügge, U.-I., and Fisher, K.**: Characterization of AtNST-KT1, a novel UDP-galactose transporter from *Arabidopsis thaliana*. FEBS Lett., **580**, 4246-4251 (2006).

36. **Zhang., B., Liu X, Qian Q, Liu L, Dong G, Xiong G, and Zeng D.**: Golgi nucleotide sugar transporter modulates cell wall biosynthesis and plant growth in rice. Proc. Natl. Acad. Sci. USA, **108**, 5110-5115 (2011).

37. **Song, X., Zhang, B., and Zhou, Y.**: Golgi-localized UDP-glucose transporter is required for cell wall integrity in rice. Plant Signal. Behav. **6**, 1097-1100 (2011).

38. **Miura., N, Ishida, N., Hoshino, M., Yamauchi, M., Hara, T., Ayusawa, D., and Kawakita, M.**: Human UDP-galactose translocator: Molecular cloning of a complementary DNA that complements the generic defect of a mutant cell line deficient in UDP-galactose translocator. J Biochem., **120**, 236-241 (1996).

39. **Aoki, K., Ishida, N., and Kawakita, M.:** Substrate recognition by UDP-galactose and CMP-sialic acid transporters. J. Biol. Chem., **276**, 21555-21561 (2001).

40. **Côté, F. and Hahn, M. G.**: Oligosaccharins: structures and signal transduction. Plant Mol. Biol., **26**, 1379-1411 (1994).

41. **York, W. S., Darvill, A. G., and Albersheim, P.**: Inhibition of 2,4-dichlorophenoxyacetic acid-stimulated elongation of pea stem segments by a xyloglucan oligosaccharide. Plant Physiol., **75**, 295-297 (1984).

42. **McDougall, G. J., and Fry, S. C.**: Xyloglucan oligosaccharides promote growth and activate cellulase: evidence for a role of cellulase in cell expansion. Plant Physiol., **93**, 1042–1048 (1990).

43. **Bilisics, L., Vojtaššák, J., Capek, P., Kollárová, K., and Lišková, D.**: Changes in glycosidase activities during galactoglucomannan oligosaccharide inhibition of auxin induced growth. Phytochemistry, **65**, 1903-1909 (2004).

44. **Beňová-Kákošová, A., Digonnet, C., Goubet, F., Ranocha, P., Jauneau, A.,**

**Pesquet, E., Barbier, O., Zhang, Z., Capek, P., Dupree, P., Lišková, D., and Goffner, D.**: Galactoglucomannans Increase Cell Population Density and Alter the Protoxylem/Metaxylem Tracheary Element Ratio in Xylogenic Cultures of Zinnia. Plant Physiol., **142**, 696-709 (2006).

45. **Seifert, G. J., and Roberts, K.**: The biology of arabinogalactan proteins. Annu. Rev. Plant Biol., **58**, 137-161 (2007).

46. **Oomen, R. J. F. J., Dao-Thi, B., Tzitzikas, E., Bakx, E. J., Schols, H. A.. Visser, R. G. F., and Vincken, J. P.**: Overexpression of two different potato UDP-Glc-4-epimerases can increase the galactose content of potato tuber cell walls. Plant Sci., **166**, 1097-1104 (2004).

47. **Qin, L.-X., Rao, Y., Li L. Huang, J.-F., Xu, W.-L., and Li, X.-B.**: Cotton *GalT1* encoding a putative glycosyltransferase is involved in regulation of cell wall pectin biosynthesis during plant development. PLOS ONE, **8**, e59115 (2013).

48. **Foster, C. E., Martin, T. M., and Pauly, M.**: Comprehensive Compositional Analysis of Plant Cell Walls (Lignocellulosic biomass) Part II: Carbohydrates. J. Vis. Exp., **37**, 1837 (2010).

49. **Brückner, J.**: Estimation of monosaccharides by the orcinol-sulphuric acid reaction. Biochemical J., **60**, 200-205 (1955).

50. **Selvendran, R. R. and O'Neill M. A.**: Isolation and analysis of cell walls from plant material. Meth. Biochem. Anal., **32**, 25-153 (1987).

51. **Yasuno, S., Kokubo, K.. and Kamei, M.**: New method for determining the sugar composition of glycoproteins, glycolipids, and oligosaccharides by high-performance liquid chromatography. Biosci. Biotechnol. Biochem., **63**, 1353-1359 (1999).

52. **Eda, S., Miyabe, K., Akiyama, Y., Ohnishi, A., and Kato, K.:** A pectic polysaccharide from cell wall of tobacco (*Nicotiana tabacum*) mesophyll. Carbohydr. Res., **158**, 205-216 (1986).

53. **Günl, M., Kraemer, F., and Pauly, M.**: The Plant Cell Wall: Oligosaccharide mass profiling (OLIMP) of cell wall polysaccharides by MALDI-TOF/MS. Method Mol. Biol., **715**, 43-54 (2011).

54. **Murashige, T., and Skoog, F.:** A revised medium for rapid growth and bioassays with tobacco tissue cultures. Physiol. Plant. **15**, 473-497 (1962).

55. **Nguema-Ona, E., Moore, J. P., Fagerström, A., Fangel, J. U., Willats, W. G. T., Hugo, A., and Vivier, M. A.**: Profiling the main cell wall polysaccharides of tobacco leaves using high-throughput and fractionation techniques. Carbohydr polym., **88**, 939-949 (2012).

56. **Mohnen, D.:** Pectin structure and biosynthesis. Curr. Opin. Plant Biol., **11**, 266—277 (2006).

57. **Eda, S., Akiyama Y., Kato, K., Ishizu, A, and Nakano J.:** Methylation analysis of cell wall polysaccharides from suspension-cultured cells of *Nicotiana tabacum*. Agric. Biol. Chem., **47**, 1783-1789 (1983).

58. **Eda, S., Ohnishi, A., and Kato, K.**: Xylan isolated from the stalk of Nicotiana tabacum. Agr. Biol. Chem., **40**, 359-364 (1976).

59. **Akpinar, O., Erdogan, K., Bakir, U., and Yilmaz, L.**: Comparison of acid and enzymatic hydrolysis of tobacco stalk xylan for preparation of xylooligosaccharides. LWT-Food Sci. Technol. **43**, 119-125 (2010).

60. **Hervé, C., Rogowski, A., Harry, J. Gilbert, H. J., and Knox, J. P.**: Enzymatic treatments reveal differential capacities for xylan recognition and degradation in primary and secondary plant cell walls. Plant J., **58**, 413-422 (2009).

61. **Willats, W. G. T., McCartney, L., Mackie, W., and Knox, J. P.**: Pectin: cell biology and prospects for functional analysis. Plant Mol. Biol., **47**, 9-27 (2001).

62. **Round, A. N., Rigby, N. M, MacDougall, A. J., Morris, V. J.:** A new view of pectin structure revealed by acid hydrolysis and atomic force microscopy.

Carbohydr. Res., **345**, 487-497 (2010).

63. **Coenen, G. J., Bakx, E. J., Verhoef, R.P., Schols, H. H., and Voragen, G. J.:** Identification of the connecting linkage between homo- or xylogalacturonan and rhamnogalacturonan type-I. Carbohydr. Polym., **70**, 224-235 (2007).

64. **Akiyama, Y., Eda, S., Mori, M., and Katō, K.**: A galactoglucomannan from extracellular polysaccharides of suspension-cultured cells of N*icotiana tabacum*. Phytochemistry, **22**, 1177-1180 (1983).

65. **Eda, S. and Kato, K.**: An arabinoxyloglucan isolated from the midrib of the leaves of *Nicotiana tabacum*. Agric. Biol. Chem., **42**, 351-357 (1978).

66. **Fry, S. C., York, W. S., Albersheim, P., Darvill, A., Hayashi, T., Joseleau, J., Kato, Y., Lorences, E. P., Maclachlan, G. A., McNeil, M., Mort, A. J., Reid, G. J. S., Seitz, H. U., and Selvendran, R. R.**: An unambiguous nomenclature for xyloglucan-derived oligosaccharides. Physiol. Plant., **89**, 1-3 (1993).

67. **Sims, I. M., Munro, S. L. A., Currie, G., Craik, D., and Bacic, A.**: Structural characterisation of xyloglucan secreted by suspension-cultured cells of *Nicotiana plumbaginifolia*. Carbohydr, Res., **293**, 147-172 (1996).

68. **Truelsen, T. A., Laird, J., and Fry, S. C.**: Xyloglucan metabolizing enzyme activities in tobacco cells. J. Plant Physiol., **154**, 95–101 (1999).

69. **Yaoi, K., Nakai, T., Kameda, Y., Hiyoshi, A., and Mitsuishi, Y.:** Cloning and characterization of two xyloglucanases from *Paenibacillus* sp. Strain KM21. Appl. Environ. Microbiol., **71**, 7670-7678 (2005).

70. **Demelbauer, U., M., Zehl, M., Plematl, A., Allmaier , G, and Rizzi, A.:** Determination of glycopeptide structures by multistage mass spectrometry with low-energy collision-induced dissociation: comparison of electrospray ionization quadrupole ion trap and matrix-assisted laser desorption/ionization quadrupole ion trap reflectron time-of-flight approaches. Rapid Commun. Mass Spectrom., **18**, 1575-1582 (2004).

71. **Yamagaki, T., Mitsuishi, Y., and Nakanishi, H.:** Structural analysis of xyloglucan oligosaccharides by the post-source decay fragmentation method of MALDI-TOF mass spectrometry: influence of the degree of substitution by branched galactose, xylose and fucose on the fragmentation ion intensities. Biosci. Biotechnol. Biochem., **62**, 2470-2475 (1998).

72. **Hsieh, Y. S. Y. and Harris, P. J.**: Xyloglucan of monocotyledons have diverse structures. Mol. Plant, **2**, 943-965 (2009).

73. **Knudson, L.**: Toxicity of galactose for certain of the higher plants. Ann. Mo. Bot. Gard., **2**, 659-664 (1915).

74. **Knudson, L.**: The toxicity of galactose and mannose for green plants and the antagonistic action of other sugars toward these. Am. J. Bot., **4**, 430-437 (1917).

75. **Yamamoto, R., Inouhe, M., and Masuda, Y.**: Galactose inhibition of auxin-induced growth of mono- and dicotyledonous plants. Plant Physiol., **86**, 1223-1227 (1988).

76. **Muñoz, P., Norambuena, L., and Orellana, A.**: Evidence for a UDP-glucose transporter in Golgi apparatus-derived vesicles from pea and its possible role in polysaccharide biosynthesis. Plant Physiol., **112**, 1585-1594 (1996).

77. **Baldwin, T. C., Handford, M. G., Yuseff, M.-I., Orellana, A., and Dupree, P.**: Identification and Characterization of GONST1, a Golgi-localized GDP-mannose transporter in Arabidopsis. Plant Cell, **13**, 2283-2295 (2001).

78. **Norambuena, L., Marchant, L., Rollwitz, P., Hirschberg, C. B., Silva, H., and Orellana, A.**: Transporter of UDP-galactose in plants – Identification and functional characterization of *AtUTr1*, an *Arabidopsis thaliana* UDP-galactose/UDP-glucose transporter. J. Biol. Chem., **277**, 32923-32929 (2002).

79. **Handford, M. G., Sicilia, F., Brandizzi, F., Chung, J. H., and Dupree, P.**: *Arabidopsis thaliana* expresses multiple Golgi-localised nucleotide-sugar transporters related to GONST1. Mol. Gen. Genomics, **272**, 397-410 (2004).

80. **Bakker, H., Routier, F., Ashikov, A., Neumann, D., Bosch, D., and Gerardy-Schahn, R.**: A CMP-sialic acid transporter cloned from *Arabidopsis thaliana*. Carbohydrate Res., **343**, 2148-2152 (2008).

81. **Reiter, W.-D.**: Biochemical genetics of nucleotide sugar interconversion reactions. Curr. Opin. Plant Biol., **11**, 236-243 (2008).

82. **Joersbo, M., Jørgensen, K., and Brunstedt, J.**: A selection system for transgenic plants based on galactose as selective agent and a UDP-glucose:galactose-1-phosphate uridyltransferase gene as selective gene. Mol. Breed., **11**, 315-323 (2003).

83. **Kohler, A., Schwindling, S., and Conrath, U.:** Extraction and quantitative determination of callose from *Arabidopsis* leaves. BioTechniques, **28**, 1086-1087 (2000).

84. **Piršelová, B., and Matušíková I.:** Callose: the plant cell wall polysaccharide with multiple biological functions. Acta Physiol. Plant., **35**, 635-644 (2013).

85. **Aoki, K., Wada, G.H.S., Segawa, H., Yoshioka, S., Ishida, N., and Kawakita, M.**: Expression and activity of chimeric molecules between human UDP-galactose transporter and CMP-sialic acid transporter. J.Biochem., **126**, 940-950 (1999).

86. **Abedi, T., Khalil, M. F. M., Asai, T., Ishihara, N., Ishida, N., and Tanaka, N.**: Expression of the human UDP-galactose transporter gene *hUGT1* in tobacco plants alters monosaccharide composition of cell wall components with hyper-galactosylation. J. Biosci. Bioeng., **121**, 573-583 (2016).

87. **Bonawitz, N. D., and Chapple, C**.: The genetics of lignin biosynthesis: Connecting genotype to phenotype. Annu. Rev. Genet., **44**, 337-363 (2010).

88. **Howell, D.C.**: Statistical Methods for Psychology Duxbury, pp. 324–325. (2002).

89. **Sewalt, V. J. H., Ni, W., Blount, J. W., Jung, H. G., Masoud, S. A., Howles, P. A., Lamb, C., and Dixon, R. A.**: Reduced lignin content and altered lignin

composition in transgenic tobacco down-regulated in expression of L-phenylalanine ammonia-lyase or cinnamate 4-hydroxylase. Plant Physiol., **113**, 41-50 (1997).

90. **MacMillan, C. P., Mansfield, S. D., Stachurski, Z. H., Evans, R., and Southerton, S. G.**: Fasciclin-like arabinogalactan proteins: specialization for stem biomechanics and cell wall architecture in Arabidopsis and *Eucalyptus*. Plant J., **62**, 689-703 (2010).

91. **Xu, S.-L., Rahman, A., Baskin, T. I., and Kieber, J. J.**: Two leucine-rich repeat receptor kinases mediate signaling, linking cell wall biosynthesis and ACC synthase in *Arabidopsis*. Plant Cell, **20**, 3065-3079 (2008).

92. **Harpaz-Saad, S., McFarlane, H. E., Xu, S., Divi, U. K., Forward, B., Western, T. L., and Kieber, J. J.**: Cellulose synthesis via the FEI2 RLK/SOS5 pathway and CELLULOSE SYNTHASE 5 is required for the structure of seed coat mucilage in Arabidopsis. Plant J., **68**, 941-953 (2011).

93. **Anterola, A. M., and Lewis, N. G.**: Trends in lignin modification: a comprehensive of the effects of genetic manipulations/mutations on lignification and vascular integrity. Phytochemistry, **61**, 221-294 (2002).

94. **Nakano, Y., Yamaguchi, M., Endo, H., Rejab, N. A., and Ohtani, M.**: NAC-MYB-based transcriptional regulation of secondary cell wall biosynthesis in land plants. Front. Plant Sci., **6**, Article 286 (2015).

95. **Ishida, N., Yoshioka, S., Iida, M., Sudo, K., Miura, N., Aoki, K., and Kawakita, M.**: Indispensability of transmembrane domains of Golgi UDP-galactose transporter as revealed by analysis of genetic defects in UDP-galactose transporter-deficient murine Had-1 mutant cell lines and construction of deletion mutants. J. Biochem., **126**, 1107-1117 (1999).

96. **Sprong, H., Degroote, S., Nilsson, T., Kawakita, M., Ishida, N., van der Sluijs, P., and van Meer, G.**: Association of the Golgi UDP-galactose transporter with UDP-galactose:ceramide galactosyltransferase allows UDP-galactose import in endoplasmic reticulum. Mol. Biol. Cell, **14**, 3482-3493 (2003).

# 公表論文

# （Articles）

(1) UDP-galactose transporter gene *hUGT1* expression in tobacco plants leads to hyper-galactosylated cell wall components

Tayebeh Abedi, Mohamed Farouk Mohamed Khalil, Toshihiko Asai, Nami Ishihara, Kenji Kitamura, Nobuhiro Ishida and Nobukazu Tanaka

Journal of Bioscience and Bioengineering, **121**, 573-583 (2016).

(2) Expression of the human UDP-galactose transporter gene *hUGT1* in tobacco plants' enhanced plant hardness

Tayebeh Abedi, Mohamed Farouk Mohamed Khalil, Kanae Koike, Yoshio Hagura, Yuma Tazoe, Kenji Kitamura, Nobuhiro Ishida and Nobukazu Tanaka

Journal of Bioscience and Bioengineering, **126**, 241-248 (2018).